Thesis Report

Automated Ultrasonic Inspection using Full Matrix Capture on Composite Materials

Richard Kruithof

Technische Universiteit Delft

TU Delft

Thesis Report

Automated Ultrasonic Inspection using Full Matrix Capture on Composite Materials

by

Richard Kruithof

to obtain the degree of Master of Science

at the Delft University of Technology.

to be defended publicly on Monday August 30, 2021 at 12:30 PM.

Student number:	1507265	
Faculty of Aerospace Engineering		
Graduation committee:	Dr. R. M. Groves,	TU Delft
	Ir. J. Sinke,	TU Delft
	Dr. A. Anisimov,	TU Delft

Contents

1 Introduction 3

1.1 Introduction . . . 3

2 Automated Manufacturing 7

2.1 Composite materials . . . 7

2.2 Manufacturing defects in fiber polymer composites. . . . 8

2.3 Automated manufacturing . . . 11

2.3.1 Filament Winding . . . 11

2.3.2 Braiding . . . 12

2.3.3 Automated Tape Lay-up . . . 12

2.3.4 Automated Fiber Placement . . . 12

2.3.5 Pick and Place . . . 13

2.3.6 Post processing. . . . 13

2.4 Summary . . . 13

3 Automated Sensing 15

3.1 Automated testing . . . 15

3.1.1 Ultrasonics . . . 15

3.1.2 Phased array ultrasonics. . . . 16

3.1.3 Radiography . . . 16

3.1.4 Eddy current testing . . . 16

3.1.5 Liquid penetrant testing . . . 16

3.2 Ultrasonic testing . . . 17

3.2.1 Ultrasonic waves . . . 17

3.2.2 Acoustic impedance . . . 18

3.2.3 Wave equations . . . 19

3.2.4 Wave propagation 19
3.2.5 Attenuation 20
3.2.6 Phased array technology 21
3.2.7 Full Matrix Capture 21
3.3 Robotics 22
3.3.1 Movement options 22
3.4 Conclusion 23

4 Research Questions and Methodology 25
4.1 Research Questions 25
4.2 Methodology 26
4.2.1 Main Research Question 26
4.2.2 Physical Integration 26
4.2.3 Data processing 26
4.3 Summary 27

5 Experimental 29
5.1 Physical components 29
5.2 Physical setup 29
5.3 Data setup 31
5.4 Experimental capture 32
5.5 ROS Integration 34
5.6 Conclusion 34

6 Results & Analysis 35
6.1 Individual FMC 35
6.2 Comparing the Data Sets 36
6.3 Enhancing the resolution 38
6.4 Analysis of the data 39
6.5 Alternative methods for data combination 42
6.6 Conclusions 43

7 Discussion 45

8 Conclusions & Recommendations 47

8.1 Conclusions 47

8.2 Recommendations 48

Bibliography 51

Nomenclature

AC	Alternating Current
AFP	Automated Fiber Placement
ATL	Automated Tape Lay-up
CAD	Computer Aided Design
CFRP	Carbon Fiber Reinforced Plastics
CNC	Computer Numerically Controlled
CT	Computer Tomography
DOF	Degree of Freedom
FFT	Fast Fourier Transfer
FLC	Fiber Laminate Composites
FMC	Full Matrix Capture
FPGA	Field Programmable Gate Array
FRP	Fiber Reinforced Polymers
FW	Filament Winding
GFRP	Glass Fiber Reinforced Plastics
NDT	Non Destructive Testing
PAUT	Phased Array Ultrasonic Testing
pre-preg	Pre-impregnated fibers
RMS	Root Mean Square
ROS	Robot Operating System
TFM	Total Focusing Method
UT	Ultrasonic Testing

Abstract

This master thesis focuses on developing an integrated system capable of performing ultrasonic phased array measurement on composite parts in an automated fashion. This could potentially be used in the manufacturing process of fiber laminate composite parts to obtain more accurate detection of manufacturing defects. Phased array ultrasonics makes use of an array of ultrasonic elements that will be used to send consecutive pulses with each of the elements which are received with the remaining elements in the array. By taking into account the signal strength of the pulses between each of the elements in the array and their respective timings a two-dimensional image of the area underneath the probe can be reconstructed into an image. This image contains information about the acoustic material properties through the depth of the measured object. By automating this method of inspection and taking consecutive measurements of this type it becomes possible to obtain volumetric data of the measured object. This research aims to investigate the feasibility and potential constraints of integrating this type of sensor system with a robotic arm. The benefit of combining this with a robot means it may be used in a repeated fashion, as well as to inspect a large number of possible geometric shapes. The final part of this thesis work will cover the processing of the data that is produced using this method.Since a large amount of data is produced, processing and analysis is needed in order to be able to visualise the data and to be able to draw meaningful conclusions from it.

1

Introduction

1.1. Introduction

Composite materials have been studied extensively since their conception in the late 1940s. It took until the 1950s to find a use in a commercial application [1]. Further applications for composite materials were discovered that stretched beyond just their lightweight properties, such as the usage of fiberglass domes to cover radio equipment due to its transparency to radio frequencies. The composite material industry has kept slowly developing until in the 1970s various resins and improved fibers were developed which resulted in the first all-composite airplanes. Starting in the 1980s fuel prices began to dominate the cost of flying and composites were starting to be used in more mainstream applications such as the horizontal stabilizer of the Boeing 737. [1]

As the knowledge about composite materials expanded so did their use in general engineering applications. Benefits provided by the use of composites are the ability to manufacture complex geometries in addition to offering impressive specific strength and stiffness properties, as well as improved fatigue and corrosion resistance compared to conventional materials such as metals, ceramics and polymers [2]. The increase in use has resulted in an increased need for reliable analysis and design methods tor the development of components. This has unfortunately not been without problems, and to this day proves to be a limiting factor in the application of composites [1].

Specific problems with composite materials have been associated with damage tolerance and detection, damage repair, environmental degradation and assembly joints. [3] The anisotropic nature of composite materials also drastically increases the number of variables that need to be taken into account when designing composite components. This combined with the fact that the base material costs as well as the processing costs of composites are higher than that of metals and plastics and this results in a higher risk of defective components [1].

In order to compensate for the cumulative uncertainties during the design and manufacturing phases of a product it is important to perform proper quality assurance steps. This is particularly the case due to the brittle nature of composites, which means that any failure mode could quickly lead to catastrophic failure of the entire part or product. This is a challenge for physical testing as it rules out destructive testing methods for reliably confirming batch properties. Instead non-destructive testing methods have been developed that can be applied to composite materials

[4].

Non destructive testing (NDT) has played a role in engineering since the 19th century when various techniques were discovered to analyze welds and later bulk materials. This was done using eddy current testing [5] and x-ray transmission testing [6] respectively. Various other techniques have been used such as liquid penetrant testing [7], magnetic particle crack detection [8] and finally ultrasonic testing (UT) [9][4].

Many of these techniques have been optimized over the last few decades, however the majority of these techniques are not applicable to modern fiber laminate composite materials (FLC). Of the NDT techniques available to FLCs there are two which are capable of imaging the bulk materials, x-ray tomography and ultrasonic testing. Of these two methods UT is the most readily available for use in the field. The increase in the use of composites has particularly affected the scale at which composites are produced. This increase in scale has led to a demand for automated testing methods. [10]

This project aims to investigate the use of advanced ultrasonic inspection methods for automated inspection in composites. Ultrasonic testing makes use of an element to induce a sound wave in the subject material, this wave will interact with the material is passes through. This wave can then be captured and analyzed to infer the state of the material it has interacted with. Ultrasonic inspection has been used for the detection of defects since the early 20th century, and is commonly used for automated inspection of parts. [11] An advanced application of UT is called Full Matrix Capture (FMC), which offers the capability to display defects through the depth of the material [12].

For an array of ultrasonic elements, each element is successively used as a transmitter, while all other elements are used as a receiver. The measurements are then stored in a matrix and used for data processing. A zone is defined underneath the array which is meshed, and for each point on the grid, the focal laws are calculated for the entire set of elements of the phased-array probe. All signals are time shifted accordingly before summation at every point of the grid. The resulting data is a section view of the material underneath the array. Compare this to traditional UT which would result in a measurement underneath the probe in the shape of a single line normal to the surface . A commonly used representation of traditional UT is a C-scan, where all measurements across a surface are represented as a surface plot. Applying the same logic to FMC it should be able to combine multiple FMC measurements across a surface into a volume plot.

In order to automate the measurements a roller-style probe will be attached to a 6 degree of freedom (DOF) industrial robot. This roller probe contains a linear array of ultrasonic elements that are submerged in water inside the silicone roller. Traditionally the entire testing setup including the probe and the sample to be measured are submerged in water to conduct the ultrasonic waves. [11] Alternatively the probe can be 'connected' to the sample through a flow of water streaming down from the probe to the sample. The roller-probe configuration aims to prevent this and requires at most a thin film of water to be applied to the sample for the silicone roller to make a good connection that allows sound waves to pass unimpeded.

The goal of this project is to develop an automated FMC system using a robotic arm and use it to collect a dataset of an aerospace grade composite. This dataset should then be analyzed to assess the coherence of the dataset, if the method is accurate enough to reconstruct the volumes and its defects.

The report is structured in the following manner: Chapter 2 gives an overview of composite materials and their manufacturing processes. Chapter 3 discusses the theory of ultrasonic testing, FMC and robotics. Chapter 4 introduces the research question and methodology. In Chapter

5 the experimental setup is laid out, and the specifications of the components used for it are provided. In Chapter 6 the results of the experiments are presented and an analysis of the obtained data will be presented. In Chapter 7 all of the results will be discussed. In Chapter 8 the conclusions are given and a recommendation for future work will be given.

2

Automated Manufacturing

This chapter discusses the manufacturing methods of composite structures. It describes the common steps in manufacturing a composite material, as well as potential defects that may arise during these processes. It then sets out to describe various automated methods manufacturing composite structures.

2.1. Composite materials

Composite materials are increasingly used to construct aerospace structures due to their excellent mechanical properties. The high specific strength and stiffness of CFRP in particular compared to conventional materials such as steel and aluminum allow for lighter structures to be created, which in turn results in the lowering of fuel requirements, and thus offering an increase in performance greater than proportional to the weight saved. The increase in performance comes with higher manufacturing costs through the need for expensive tooling, high raw material costs, the need for high temperatures and pressures when processing the material, and high wear it imposes on the tools used to cut the final structure to its final dimensions. Consequently there is a great need for inspection of fabricates early in the production process to identify problems which may have occurred anywhere during the production. This section will explain what composite materials consist of and how they are constructed in order to provide background information towards how they can be inspected.

Composite materials take their name from the combination of two or more materials, and they can consist of a wide range of materials in various form factors. A composite material can tailor its mechanical properties based on the properties of the subcomponents used to construct it, but more importantly, it can tailor its mechanical properties dependent on the direction the material loaded in. This allows for intelligent design of the structure where the material is most effective in the directions that matter. As such, a composite material could already be considered a structure by itself.

The type of composite most commonly used for aerospace structures are fiber reinforced polymer laminates. These are made of sheets of the fibrous materials, often woven or stitched into textiles to be placed on the tooling, but may also be applied to the tooling directly as smaller tapes or yarns. The process of applying the fibers to the tooking is referred to as the lay-up process. These layers of fibers will then all be interconnected through a polymer, which is referred to as the matrix. The matrix will ensure the material keeps its intended shape once the polymer has cured, and will transfer shear forces between the fibers.

The matrix may have been applied to the fibers in advance, known as pre-impregnated fibers or pre-pregs. Pre-pregs are often tacky at room temperature, until the resin is cured in an oven or autoclave. Liquid resim may also be applied to the dry sheets of fibers before it is applied to the tooling, which is called wet lay-up. The resin may also be injected into the fibers with the use of either vacuum pressure, overpressure, or a combination of the two.

Besides fiber polymer laminates other topologies of composite materials can used, such as short fiber laminates, bulk fiber injection materials, and even fiber metal laminates. Fiber polymer laminates may also be used in combination with low density foams or honeycomb materials to create sandwich structures. The foams typically consist of polymers, and honeycomb typically consists of aluminum or aramid. Metal and ceramic composites also exist, but they are usually limited to meet extreme temperature requirements, such as space applications.

The scope of this research will be limited to fiber polymer laminates, as those make up the majority of aerospace applications [13]. In order to assess the types of defects that may be introduced during the manufacturing of these laminates, the production steps will be laid out.

2.2. Manufacturing defects in fiber polymer composites

There are several methods to create composite laminates, but each of these will have a number of steps in common. A detailed description of each of these steps can be found in the literature study. [14] Various defects may be introduced during each of these steps, and they are summed up in table 2.1.

Table 2.1: Summary of production stages and defects that may be introduced

	voids	delamination	inclusions	matrix cracking	fiber tear-out
mould preparation			x		
lay-up			x		
pressurization	x	x			
resin infusion	x				
consolidation		x		x	
mould release		x		x	
post processing		x		x	x

The smallest size at which these defects occur lies in the order of magnitude of micrometers. In figure 2.1 microscopic images are shown that display examples of these different flaws. These images were taken from a number of samples encased into a slug that was prepared for microscopic imaging, this slug is displayed in sub-image 1. Image 2 displays pristine a cross-section of fiber laminate material. Image 3 displays cracked matrix due to mechanical forces, from the image it can be seen that the matrix has lost mechanical attachment to part of the fiber, reducing the load transfer capability between the fibers and the matrix. Image 4 displays what the material looks like after fiber-tear-out has occurred. Images 5 and 8 display voids at different magnifications, these voids may be filled with either air or vacuum depending on whether the discontinuity connects to the outer edge of the material. Images 6, 7, 9 and 10 display what the fiber material looks like after failure was induced due to mechanical loading.

What can be seen from these images is that these flaws occur at a scale of 10’s to 100’s of micrometers, which can be used as a reference in analyzing the results of ultrasonic imaging techniques. If the size of these flaws is smaller than the resolution of the imaging techniques then the flaw would go undetected. The impact of these flaws is difficult to quantify, as composite laminates are brittle in nature. Failure may occur at a microscopic level without significantly affecting the mechanical behavior of the material until the failure has grown to a significant enough size to where it causes catastrophic failure of the structure.

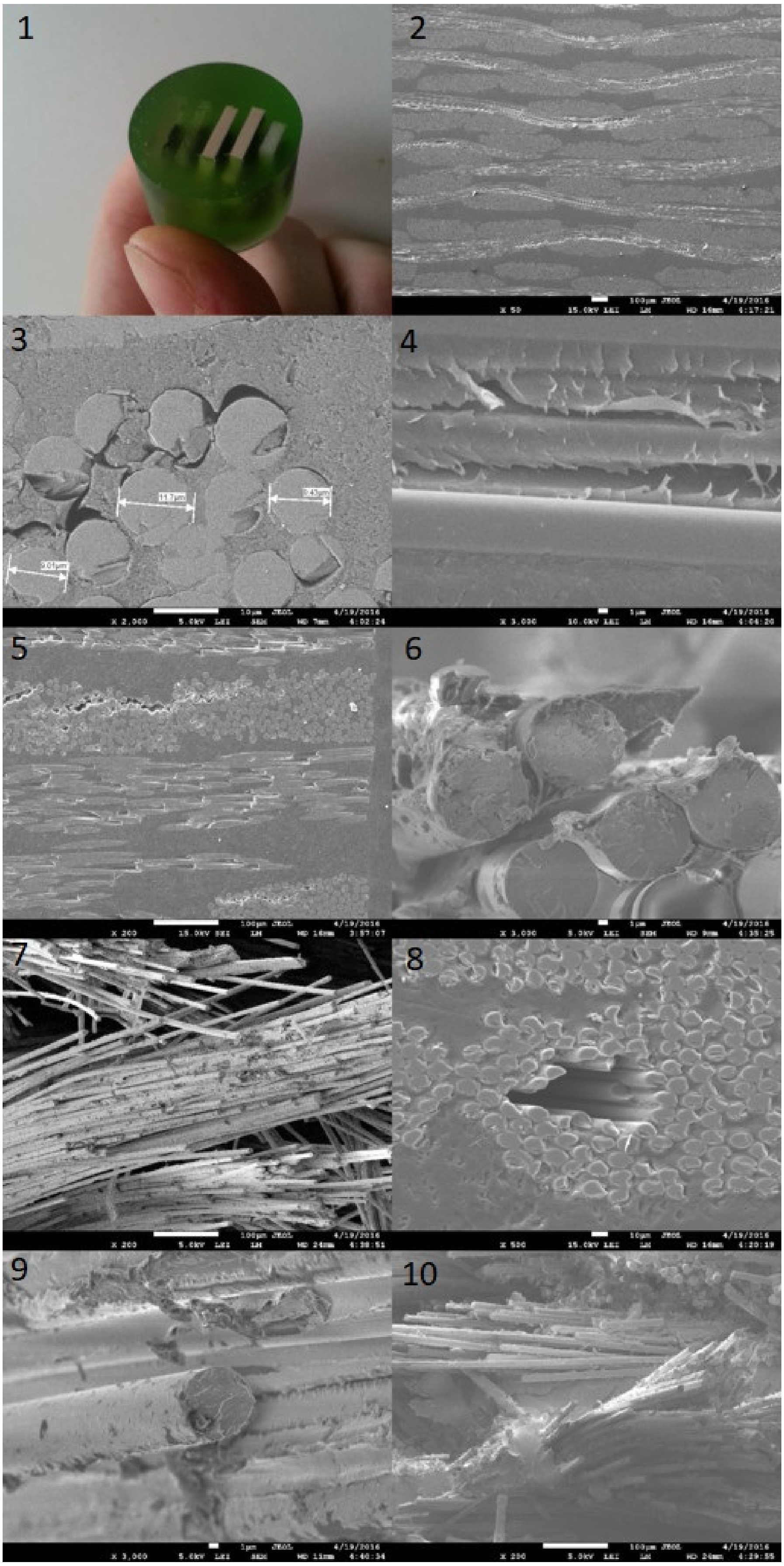

Figure 2.1: Microscopic imaging of composite laminates. These images were taken during the Trinity Excercise

2.3. Automated manufacturing

Automation is the mechanization of work to replace manual labor and even reduce human-machine interaction [15]. Machines have the benefit of being able to operate consecutively and for long periods of time, while offering high levels of precision and repeatability in their operation. This has resulted in a drastic increase in production speeds and production volumes, which has particularly benefited the production of composite structures as their manufacture can be very labor intensive and therefore time consuming. The methods that are currently used for automated composite production are [16]:

- Filament Winding (FW)
- Braiding
- Automated Tape Layup (ATL)
- Automated Fiber Placement (AFP)
- Pick and Place

These methods are used to produce the basic composite structure, which may be further refined with machining tools to trim the product to its final proportions. This machining step can be automated as well, when performed by Computer Numerically Controlled (CNC) lathing and milling machines. [17] It may seem inefficient to produce oversized composites, only to trim them down to their final dimensions later. This however ensures that the edges of the composite are flat and uniform. Internal forces that arise due to the anisotropic nature of composites are resolved at the edges, and it is therefor of importance to ensure that these surfaces are of sufficient quality. [18]

2.3.1. Filament Winding

Filament winding is a method that is used to create axisymmetric parts, as well as some non-axisymmetric parts. A machine head is usually mounted on a carriage which can travel along the length of the product as well as perpendicular to it. It operates very similarly to a CNC lathe, with the difference that the machine adds material with each pass, rather than removing it. FW makes use of tapes or tows of composite material which are fed from a programmable machine head onto a spinning mandrel under tension. These tows can hold up to 24k filaments, and individual tapes are generally around $3mm$ wide. Generally 5-10 tows are laid simultaneously as they are led across the mandrel surface parallel to another. [16]

Much like manual lay-up filament winding may be done with either pre-preg composite tapes, or with dry fibers that are to be impregnated at a later stage. An additional option presented by filament winding is wet winding, where the dry fibers are run through a resin bath shortly before they reach the mandrel. The speeds of the carriage that feeds the fibers is matched with the rotating speed of the mandrel to create different winding patterns. These may be hoop patterns, polar winding patterns or various helical patterns, resulting in different principal directions of the fibers. [19]

Voids are relatively common in filament wound composites compared to other automated production methods. [19] This has been attributed to the undulations of the fibers which is caused by them traveling over and under tows as they are being wound onto the mandrel. This effect is less prominent with pre-preg slit tapes, as they produce a flatter surface while being wound.

Filament wound plies do suffer from a small degree in variation of their mechanical properties across the laminate, as unlike a woven layer the ply is slightly unbalanced around the midplane with FW.

2.3.2. Braiding

Braiding is similar to filament winding in the fact that fibers are pulled under tension onto a rotating mandrel [20]. However rather than applying a single bundle of tows it can feed a large number of them distributed over the circumference of the cross-section. This allows a braiding machine to reach feed-rates almost an order of magnitude higher than FW machines. A downside compared to FW may be the limitation of patterns that are possible with braiding. Because a higher number of tows are placed simultaneously the maximum fiber angle with respect to the longitudinal axis that can be achieved without overlapping is significantly lower. These hoop windings are particularly important for pressure vessels, which may make the FW process preferable for such parts.

2.3.3. Automated Tape Lay-up

Automated tape lay-up (ATL) [21] machines lay tapes of composite material onto a mould surface. The process is suitable for both thermoset pre-preg composites as well as thermoplastic composites and makes use of tapes ranging in width from 75-300 mm. A machine head is equipped with the following components:

- Spools of material
- Winder
- Winder guides
- Compaction shoe/roller
- Tape cutter
- Position/Pressure sensor

This machine head may then be either attached to a gantry, or onto a robot cell.

The ATL machine operates by moving the head across the mould surface, applying tape in specified directions. Thermoplastic tape laying machines may include a heating element to melt the polymer matrix, bonding it to the substrate as it is being laid. For pre-preg composites the benefit of this process is that the compaction step is being performed during the lay-up stage. Depending on the configuration this may remove the need for intermediate debulking cycles. ATL can be very cost efficient when it comes to lean manufacturing, however the ATL machine itself may require a signifcant capital investment.

2.3.4. Automated Fiber Placement

Automated fiber placement (AFP) serves the same function as ATL, as its lays up to 32 individual tows or tapes onto a mould surface. The main difference comes from the material used for the process, as the tapes used in AFP are similar to those used in FW with a width of approximately $3mm$ [21]. AFP also has the ability to cut individual tapes, as well as stop and start dispensing them mid-process. In addition to this individual tapes can be fed at different rates, making it much more suitable for placing tapes around a radius. The limitation of this radius follows from the maximum radius a tape can be sheared over before it will buckle.

The major limiting factor of AFP is the minimum length of tows the machine can place. This minimum tow length is a result of the distance between the roller and the cutter. If the trailing edge of the tow is cut before the leading edge has been pinched by the roller it will just fall down.

2.3.5. Pick and Place

Pick and place technology is a novel technology that uses a machine to grab on to a composite textile, and position it on the mould. It may use either grippers that grab the edge of the fabric, or distributed vacuum grippers that use suction to hold on to the fabric. It can be classified into two categories, 2D to 2D and 2D to 3D handling, referring to the geometries of the textile before and after placement. The most interesting of these is the 2D to 3D handling, which can be used to pick up plies and place them over the mould. Unfortunately this technology has not yet reached the level of maturity where it can be implemented in production [22]. 2D to 2D handling may be more feasible in the short term, which may be used to form a stacked fabric.

Over the last few years a lot of research has been done in this area though, as there are multiple interests for such a technology. A large portion of current research focuses on the placement of dry fibers, while the rest of the research work is divided into the placement of pre-pregs, thermoplastic composites, and auxiliary materials. The automatic placement of auxiliary materials such as peel-plies, bleeder material, breather material offers great prospects as it can be used for both dry fiber processes as well as pre-pregs. [22]

2.3.6. Post processing

When a composite product has finished the curing stages it is still oversized compared to the final product dimensions and needs to be trimmed down. In an automated production setting this is most commonly done with 4-6 axis CNC machining. More degrees of freedom for the CNC means more freedom for the component geometry, and generally 5-axis CNC's are used in order to reach all edges of the product. The CNC is used to perform drilling, milling and sometimes lathing operations on the product. Tool wear is of specific concern when machining composites, as the surface hardness of CFRP products is very high. Worn tools are a common cause for delaminations and torn fibers, so special tools are often used for machining CFRP that are more resistant to wear [23].

2.4. Summary

There are multiple automated production methods employed for the production of composite materials, which have resulted in a significant increase in production volume compared to manual methods. This increased production volume means it has become less feasible to perform manual inspections, resulting in an increased need for automated testing.

Chapter 3.2 will provide some more insight in ultrasonic inspection methods and the additional information provided by phased array systems.

3

Automated Sensing

This chapter discusses damage detection methods and ways they are automated. It goes more in depth on the theory of ultrasonic sensing and provides an explanation of phased array ultrasonics and the Full Matrix Capture method. It then discusses robotics and the way they are used.

3.1. Automated testing

Current methods that are being used to perform structural integrity tests include ultrasonics, radiography, eddy current testing, magnetic particle testing, computed tomography scanning (CT), visual inspection, and liquid penetrant testing [4, 24, 25]. Depending on the situation, laser sensing may also be used to determine the lay-up quality during layup [26]. Not all of these are suitable for automated testing however, and only a few of these are seen in automated NDT systems used for industrial aerospace components. The sections below describe the published applications of automated sensing for composite inspection.

3.1.1. Ultrasonics

Automated ultrasonic scanning systems have been widely popular in industrial applications due to the large amount of information they provide, as well as allowing for in-situ inspection [27]. Automated UT is often used to perform C-scans, which provides a representation of the scan data in a plane parallel to the scanned surface. [11] Because of this the entire product can be scanned with a single pass which is beneficial in a production environment where the speed of scanning is considered an important factor. A major hurdle in the automation of ultrasonic testing methods is a proper conduction of the acoustic waves between the specimen and the probe. This problem is normally approached by submerging the object to be scanned in a tank filled with water, or using a stream of water between the probe and specimen to conduct the waves. In 2010 a CO2 laser based ultrasonic system was used to perform inspection on aerospace components with a 6 axis manipulator [28], avoiding this issue altogether. In 2015 the use of a robotic arm in combination with optics and ultrasonics was used to perform part recognition [29]. The result of their work allows the system to identify and classify unknown parts into a machine interpretable format, which removes the need of a Computer Aided Design (CAD) model of the part that is to be scanned.

3.1.2. Phased array ultrasonics

Phased array ultrasonics (PAUT) appears to be a straightforward upgrade from conventional ultrasonic testing since it contains multiple transducer elements, which offer it a set of additional features without sacrificing any existing ones [30]. In 2013 a 16-element PAUT sensor was mounted to a robotic arm to perform automated scanning of a planar surface [31]. This work focused largely on the validation of the test results of a moving sensor and interpretation methods of the data. In 2016 a method was developed to use PAUT to significantly increase the attainable measuring speeds [32]. The focus of their research was predominantly in the exploitation of the PAUT's property of carrying multiple piezo elements to perform concurrent measurements. They were able to achieve scanning speeds of 18.1 m^2/hour, and by utilizing the elements concurrently they reached scanning speeds of 117.6 m^2/hour. In their work they acknowledge the potential of using FMC to improve the results, but do not provide any results associated with it.

3.1.3. Radiography

Radiography can be a reliable form of inspection, given that the component is suited for this method [33]. The most commonly used method of radiography is x-ray inspection, in which electromagnetic waves are transmitted to the specimen and are captured after passing through the material. A downside of this method is that for increasingly thicker parts the amount of energy required to penetrate the matter increases exponentially. Furthermore composites express a low level of x-ray absorption, making the technique difficult to apply on these materials. This may however be used as an advantage when inspecting sandwich composites made with metal honeycombs, allowing the method to focus primarily on the internal parts of the structure [6]. Such measurements must be performed in an environment where the operators are shielded from the radiation emitted by the scanning device, which is often a secure room. This means that radiography may not readily be used for on-site inspection.

3.1.4. Eddy current testing

Eddy current testing is a popular method to find surface cracks in a structure, although it is also capable of corrosion detection with proper configuration [5]. The method uses a coil powered with alternating current (AC) to generate an electromagnetic field that induces currents in the specimen. These induced currents will be flowing in a loop, and will cause mutual inductance with the probe which can be used for measurement. Unfortunately the sensitivity to surface cracks with this method relies on the conductivity of the specimen. This means that for glass fiber reinforced polymer (GFRP) laminates this method is completely ineffective, as they are not conductive of electricity. CFRP is a semiconductor, and as such this method will work, however the electrical conductivity is not uniform throughout a laminate and may interfere with measurements. [34]

3.1.5. Liquid penetrant testing

Liquid penetrant testing is a method that is used for the detection of surface defects [7]. Although not entirely unsuitable for automation, this method does involve a lot of manual work in preparing the specimen. Automated analysis of results from liquid penetrant testing may be evaluated by using photographic images. [35] This attempts to remove some of the uncertainty of the method by comparing the computerized results with a database to make a more accurate prediction of the material properties.

3.2. Ultrasonic testing

To take an ultrasonic measurement a short pulse of mechanical energy needs to be transmitted to the material's surface to induce an elastic wave within the material. [9] This wave will typically be in the megahertz frequency range depending on the wave propagation velocity (V) of the material. A proportion of this wave will be reflected off of discontinuities within the material, see figure 3.1. In a variation on this method a resonant mode of vibration is induced within the material and defects are detected by shifts in the resonance frequency or changes in the damping of the signal.

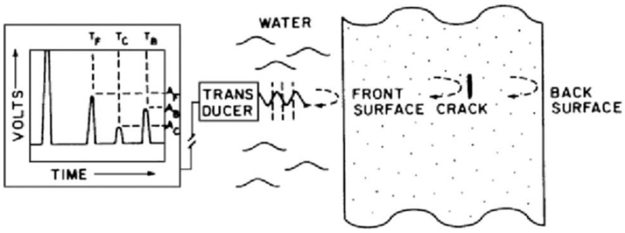

Figure 3.1: Schematic representation of an A-scan resulting from a pulse echo measurement. [36]

Ultrasonic waves are generally induced by transducers consisting of a piezoelectric element sandwiched between a surface layer and a damping layer. When the piezoelectric element is excited with the use of an electrical pulse it will contract and expand according to the principles of piezoelectricity. This will cause it to transfer a mechanical pulse into the material or an intermediate coupling agent. The ultrasonic signal is retrieved in a similar manner in which they were induced, using a reciprocal process of the piezo element where it converts the mechanical waves back into electrical charge which can be measured. [37]

This technique requires a physical coupling between the measured part and the piezo element, this is typically done by either submerging the part in a water bath or applying a coupling fluid between the transducer and the material. [11] This need for coupling may introduce some problems which could limit its applications for instance on moving parts or at elevated temperatures. Certain probes have been developed to circumvent these problems. In this project we will be attempting to move a probe along a surface material, which proves a challenge with conventional piezo-transducer probes.

The probe that is selected for this project is specified in chapter 5, but it gets around this problem by containing the transducers within a silicone shell that is filled with water. This silicone shell only needs a small amount of water applied externally to couple with the material. A downside of this configuration is that the pulse will transfer through water, followed by a region where it will transfer through silicone followed by the material. The lack of a sharp transition in acoustic impedance means that the resulting front wall signal becomes less distinct, making it difficult to properly observe the material properties of thinner samples.

3.2.1. Ultrasonic waves

A sound wave or ultrasonic wave corresponds to the transport of mechanical energy in the form of particle movement [11]. Movements transmitted between atoms are referred to as transient waves, and can be propagated in solids, liquids and gases. Depending on the attenuation of the material the wave will travel a certain distance over which it will accumulate a loss in energy. The amplitude A of a wave is propagated through a material according to the following relationship:

$$A = A_0 cos(2\pi f - kr) \tag{3.1}$$

Where A_0 is the initial amplitude, f is the frequency, k the wavenumber, and r is the distance. Using period T, wave velocity V we can respectively define the pulse ω, wavelength λ and the wavenumber as:

$$\omega = 2\pi f = \frac{2\pi}{T}[rad/s] \tag{3.2}$$

$$\lambda = \frac{V}{f}[m] \tag{3.3}$$

$$k = \frac{\omega}{V} = \frac{2\pi}{\lambda}[rad/m] \tag{3.4}$$

It is worth noting that for a measurement conducted with a piezoelectric transducer the waves will be composed of multiple frequencies defending on the specific transducer. In order to characterize a material it is considered standard practice to measure the time period of the signal to deduce the velocity. The signal is observed in the time domain, but can be converted to the frequency domain using a Fast Fourier Transform (FFT). Both of these representations for a signal with a central frequency of $f_c = 250Hz$ traveling through concrete are depicted in figure 3.2.

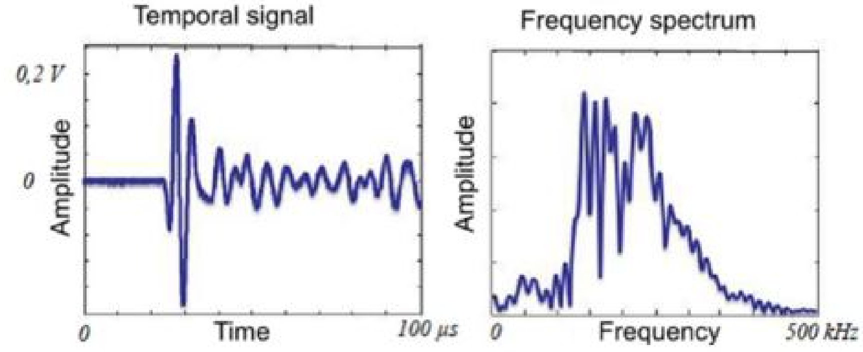

Figure 3.2: Time and frequency signal of an ultrasonic wave with central frequency $f_c = 250Hz$. [9]

3.2.2. Acoustic impedance

An ultrasonic wave experiences resistance as it passes through a material. This resistance is a property of the material and is referred to as acoustic impedance. This value represents the ratio of acoustic pressure to the vibration velocity of particles at a given point. For solid materials this value can be calculated from the material's density (ρ) and ultrasonic wave velocity V.

$$Z = \rho V[kgm^{-2}s^{-1}] \tag{3.5}$$

The values of acoustic impedance of commonly used materials in aerospace engineering are listed in table 3.1. The reflection and refraction of ultrasonic waves are a property of changes in acoustic impedance a wave encounters as it passes through an object.

Table 3.1: Acoustic properties of various materials [38]

Material	Acoustic Impedance (Z [kg/m^{2}s])	Density (ρ [kg/m^3])	Wave Velocity (V [m/s])
Air	426	1.29	330
Water	$1.5 \cdot 10^6$	1000	1480
Aluminium	$13.5 \cdot 10^6$	2700	6320
Steel	$45 \cdot 10^6$	7810	5800
GFRP	$3.8 \cdot 10^6$ - $5.5 \cdot 10^6$	1400-1990	2740
CFRP	$4.8 \cdot 10^6$ - $5.5 \cdot 10^6$	1550-1800	3070

3.2.3. Wave equations

A set of equations is written using Hooke's law and the principles if dynamics for when effort is applied to a particle over time. The general equation for wave propagation is given by the displacement field u in the environment in which a wave is propagated. [9]

$$\rho \frac{\partial^2 \bar{u}}{\partial t^2} - (\lambda + \mu)\overline{grad}[div(\bar{u})] - \mu \Delta \bar{u} = \bar{0} \tag{3.6}$$

Where ρ is the density and λ and μ are second order coefficients of elasticity of the material, called Lamé coefficients. If this set of equations is solved the particle displacement $\bar{u}$ can be broken down into longitudinal compression wave potential (scalar φ) and transverse shear wave potential (vector $\bar{\zeta}$). The two wave potentials in $\bar{\zeta}$ are polarized and are perpendicular to each other. The waves associated with these potentials are used to check Helmholtz equations which results in the following propagation speeds deduced from the general equation.

$$V_p = \sqrt{\frac{E(1-\nu)}{\rho(1+\nu)(1-2\nu)}} \tag{3.7}$$

$$V_s = \sqrt{\frac{E}{2\rho(1+\nu)}} \tag{3.8}$$

Where V_p and V_s represent the velocities of the compression (pressure) waves and shear waves respectively as a function of the mechanical properties of the material, where E is the elastic modulus, ν is the Poisson's ratio and ρ is the density. These waves are also referred to as longitudinal and transverse waves.

3.2.4. Wave propagation

In the application of ultrasonic techniques wave propagation is typically reduced to a one-dimensional problem. This allows for the assumption of plane waves to propagate. As depicted in figure 3.3 compression wave propagate in the same direction as the wave propagates where transverse wave move perpendicular to the direction of propagation. The two transverse waves U_{t1} and U_{t2} represent motion perpendicular to each other, and their respective sensitivities can be affected by the directional properties of anisotropic materials.

In addition to these two types of waves there will also be waves propagated along the surface.

Depending on the thickness of the material that is impacted and the energy of the impact either a raleigh wave or a lamb wave will be created. These waves will take the majority of the energy and dissipate it in the material. For the methods applied in this project only compression waves will be used.

This theory is applicable for planar waves in homogeneous isotropic elastic liniar materials, which means that for fiber laminate composites (FLC) some additional analysis is required on how the heterogenous nature of FLCs affects UT measurements. This will be addressed in detail in section 2.1

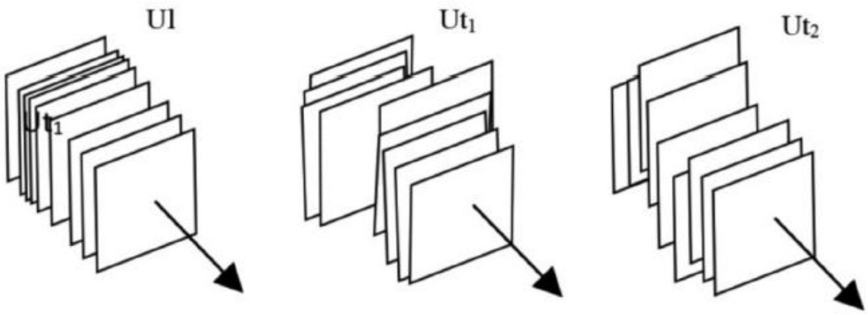

Figure 3.3: Direction of propagation and wave motion for longitudinal (U_l) and transverse ($U_{t1,2}$)waves [9]

3.2.5. Attenuation

As ultrasonic waves propagate through a material they are submitted to attenuation. Attenuation α_{US} [DB] is defined as the loss in amplitude between two successive echos A_1 and A_2 over distance ΔL [9]:

$$\alpha_{US} = \frac{20}{\Delta L} log \frac{A_1}{A_2} \tag{3.9}$$

Attenuation is a result of geometric divergence, dissipation, dispersion and diffusion [9]. Geometric divergence occurs as the wave propagates through the material in a conic shape, expanding the wave surface over a larger surface as it travels further, thus reducing the wave energy available per unit surface area. Dissipation occurs as a result of friction within the material, converting the mechanical energy into heat energy. Dispersion occurs in heterogeneous materials, and causes the signal to be distributed over a wider range of frequencies. This causes the wave velocities within the material to diverge as the wave propagates through regions with different impedance. Diffusion occurs due to heterogeneity within a material, as a wave interacts with local increases or decreases in acoustic impedance the wave will reflect off of these regions re-emitting a fraction of the incident wave energy. As a result the amplitude of the wave traveling in the direction of the incident wave will reduce. Whether this process occurs depends on the size of the anomalous regions, their density, and the differences in acoustic impedance. Diffusion reaches a maximum level when the source of the diffusion has a similar size to the wavelength. Since composite materials are laminar in nature this means a wave frequency must be chosen for which the wave does not disperse or diffuse as a result of the wave crossing between plies. For this reason a typical frequency that is chosen for measuring CFRP is $5 MHz$.

3.2.6. Phased array technology

Phased Array Ultrasonic Testing (PAUT) expands upon conventional ultrasonics by operating arrays of 2^N piezoelectric elements typically organized in a linear fashion. These elements can be actuated individually, in phase with each other or with a specific phase delay. This allows for a wavefront to be transmitted in a non-perpendicular direction to the surface. The parallel use of these elements can be used to increase the observed area per measurement, thereby increasing the speed with which measurements are taken. A technique called Full Matrix Capture (FMC) can be used to obtain a perspective image of the acoustic properties underneath the probe [39].

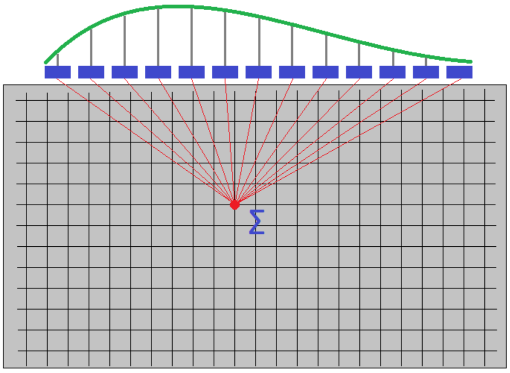

Figure 3.4: Calculation of combined signal at a node on the grid

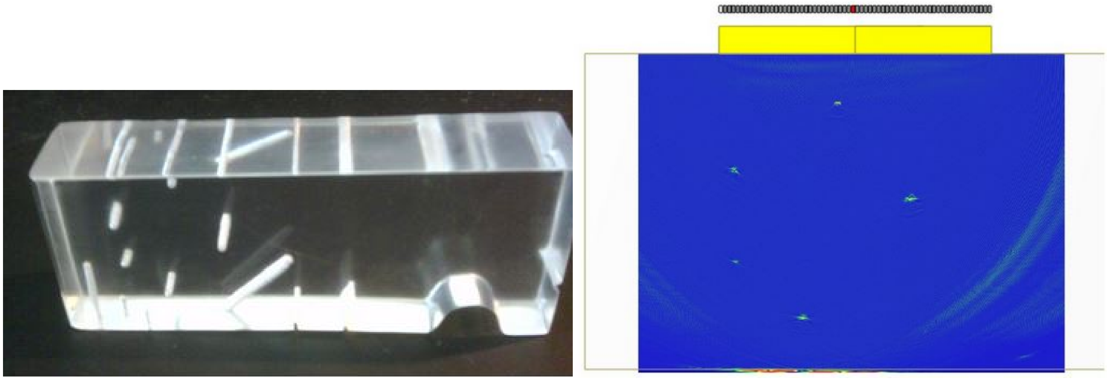

(a) Sample of rexolyte polymer

(b) processed FMC of the sample

Figure 3.5: Sample FMC of homogenous material [12]

3.2.7. Full Matrix Capture

Full Matrix Capture is a data-acquisition process using phased-array probes. For an array with N elements, each element successively transmits while all other elements receive. As a time-signal is captured for each of these combinations of elements they can be stored in a matrix of NxN dimensions. This matrix can be used for data processing, a signal processing operation called the Total Focusing Method (TFM) is applied. A geometric zone underneath the probe is defined within the material for reconstruction. This zone is meshed with a grid of nodes, and for each of the nodes the focal laws are calculated for each of the PAUT elements. Again for each of these nodes each signal in the matrix is time shifted according to these focal laws before summation. When this process has been repeated for each of the nodes the reconstruction is done. See figure 3.4 for a schematic representation of the calculation, figure 3.5 for an example of FMC applied to a homogeneous material and figure 3.6 for an example of FMC applied to a CFRP laminate.

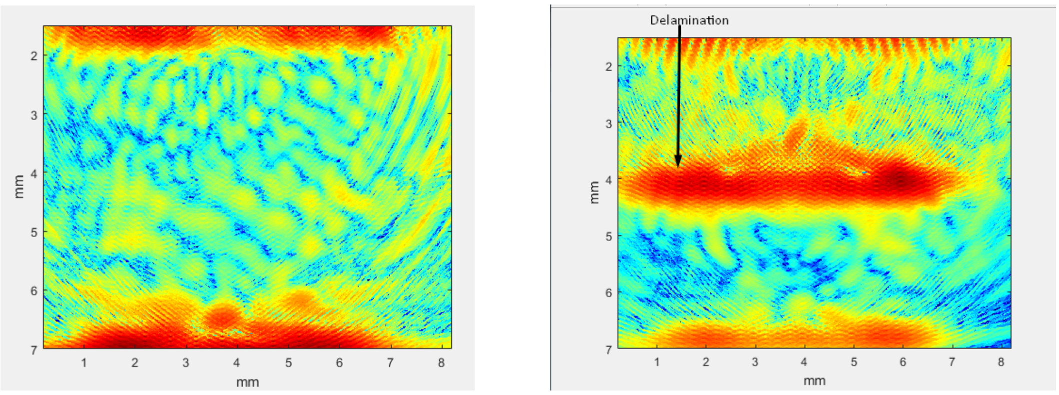

(a) FMC measurement of a CFRP sample without any delaminations

(b) FMC measurement of a CFRP sample with a delamination present

Figure 3.6: FMC measurements of a CFRP sample

3.3. Robotics

The position control of the ultrasonic probe is proposed to be performed with a robotic cell. There are several aspects of robotics that are relevant to discuss.

3.3.1. Movement options

Robotic cells consist of several joints which allow rotation around the axis of their shaft, linked together by elements of a certain length in order to create a planned movement of the final joint. The proposed robot as displayed in figure 3.7 is a 6 degree-of-freedom (DOF) robot that allows for translation and rotation in all 3 cardinal directions. Movement of a robot can be thought of as the combination of rotational and translational movement of the final joint, which is attached to the tooling the robot is used to operate. [40] Software is used to calculate the movements of all of the joints in order to obtain the correct movement of the final joint. [41] These movements are calculated based on an input command, which can be a linear movement of the final joint, a designated rotation of a specific joint, or rotation of the final joint around a fixed point in space.

The robot operates in a workspace within which it has the reach to operate the tooling, this workspace usually contains a flat surface on which objects can be mounted for the tooling to operate on. This surface is also called the bed, and the object that is attached to the bed and is to be operated on by the tooling attached to the robot shall be called the sample. The robot is constrained in its movement so it is unable to extend outside the designated workspace for operational safety.

The movement of the robot may need to be controlled based on more than just the position of the final joint. When tooling is attached that needs to make physical contact to an object fixed on the bed it may be necessary to control the force which is applied between the two. In order to control this a sensor can be added to the robot which measures the force applied and can control the robot position accordingly in order to keep this pressure constant. The precision with which this needs to be done depends on the relative stiffness of both the tooling and the sample,

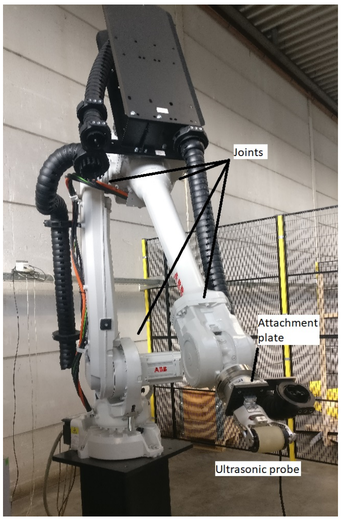

Figure 3.7: A picture of the ABB IRB4600 robot proposed to be used for the measurement configuration. Attached to the final joint is the ultrasonic probe.

the higher the stiffness the more accurate this needs to be [42].

The combination of angles of each of the joints and resulting position of the end effector is referred to as the pose of the robot. This pose of the robot is tracked and logged using a software system that can communicate these values over a network, which in the case of this robot is done through ROS [43]. This system will communicate at an interval in the millisecond range depending on the configuration of the system. This system is modular and can be accessed by additional hardware such as a probe attached to the robot, and can be used to transmit the data from the probe across the network integrated with the corresponding position data at which measurements are taken [43].

The control of the robot can be done in two separate ways, either by direct and realtime control of the separate axes of the robot, or by programming a path for the robot to travel. In the latter case, each of the axes will be calculated in order to accommodate the planned movement, and once the movement has been programmed it can be used and repeated at will.

The accuracy of the sensor positioning using the robot can be expected in the range of $0.5mm$ [44], which may pose a limitation on the measurements. Depending on the speed at which the robot is moving the accuracy may increase or decrease, which means that when taking measurements the probe should not be moving too fast.

3.4. Conclusion

This chapter discussed the background information necessary for integrating the ultrasonic sensor system with a robotic cell to be used to scan for flaws in a composite materials. The first section discussed the different applications of ultrasonic testing and in particular Full Matrix Capture. For the experimental setup FMC is proposed since it provides detail about the material properties across the depth of a measured panel. The second section discussed composite materials and the different manufacturing defects that can occur. This section concludes that defects as small as 10s to 100s of micrometers can be found to occur within these materials. The ultrasonic measurement techniques have a resolution that depends on the wavelength of the ultrasonic pulses used, however the material also attenuates waves propagating through the material that have a frequency too far from the resonance frequency of the material. This leaves a narrow range of frequencies available for use on composite materials. The final limiting factor of the precision of measurements is the accuracy of the robot movement, depending on the speed and distances the robot has to travel this precision can vary with an upper limit in the order of $0.5mm$.

4

Research Questions and Methodology

In this chapter the research questions will be presented that this research tries to answer. It also includes the methodology, which explains why the question is asked and how it will be attempted to be answered.

Chapter 2 discusses methods of manufacturing composite materials. In this chapter potential defects that may be introduced during the manufacturing process of these composites are identified. Chapter 3 discusses methods of inspecting materials for damage. It reaches the conclusion that ultrasonic testing is a powerful tool for nondestructively identifying flaws in a material which can be used in the field. It observes that currently ultrasonic inspection is already an effective method for automated inspection, and that recent advances in ultrasonic testing have made it possible to obtain more detailed images of material. This has resulted in the idea of automating FMC in a similar way regular UT is already being automated. This should provide the benefit of offering more detailed information about the measured material at the expense of having to work with a much larger volume of data.

4.1. Research Questions

The overall research question that is to be covered by this research is the following:

- Can automated FMC be used to inspect composite parts?

This research question can be divided into two sub questions:

- Can FMC be used in conjunction with Robotics to scan fiber laminate composite materials?
- Can orthogonal datasets be used to improve the probability of detection of FMC data measured of composites?

4.2. Methodology

This section will describe the reasoning behind why the research question was chosen and method by which the research question will be answered.

4.2.1. Main Research Question

The main question of this research is: ”Can automated FMC be used to inspect composite parts”. This question originates from the fact that automated ultrasonic inspection is already widely used for quality control in manufacturing of composite structures . The most common implementation of this is C-scans for the inspection of objects with large surface areas. On the other hand advances have been made in ultrasonic capturing techniques, including FMC and TFM to reconstruct these measurements into image that provides information about material properties through the thickness of the material. In part due to the novelty of the technique this has not yet been widely implemented in automated inspection solutions yet. Automated inspection using FMC have been proven to be feasible in prior research, but has only been done for isotropic materials.

Between isotropic materials and fiber reinforced polymer (FRP) materials a large difference in the output of FMC can be observed, as can be observed in Figures 3.5 and 3.6. Measurements on isotropic materials have a much lower variation in background signal level than those on FRPs. As a result it is more difficult to distinguish between background variations and actual defects. This translates to a reduced probability of detection for defects in FRPs, meaning flaws which could affect the structural properties of a material may go undetected.

4.2.2. Physical Integration

The first sub question of the research question is: ”Can FMC be used in conjunction with Robotics to scan fiber laminate composite materials?” This question focuses mainly on the physical aspect of the integration. The first part of trying to answer this question is done by trying to create a configuration where a sensor capable of taking ultrasonic FMC measurements is combined with a robotic arm. This implies not only the physical attachment of parts, but also the integration of digital systems. The goal here is to create a system that integrates the pose tracking of the robot with with measurements taken by the sensor to obtain data with their relative position data attached.

Other aspects of the physical integration are the selection of components in order to assure compatibility of the systems. An example of this would be the selection of a roller-type ultrasonic probe compared to a direct contact probe, but may also include other required components such as pressure sensors for the robot.

4.2.3. Data processing

The second sub question of the research question is: ”Can orthogonal datasets be used to improve the resolution of FMC measurements of composites?”. The aim is to create a 3-dimensional dataset in a cartesian grid which contains the calculated acoustic impedances of an entire volume of material.

This question tries to deal with the high level of variation measured in the background signal level of ultrasonic FMC measurements when processed using the TFM algorithm. One feature of FMC measurements is that they contain a high level of detail in one plane as seen in Figure 3.6. When taking several of these measurements with a normally acceptable spacing there will be a large disparity in resolution in the direction normal to the plane of measurement compared to the resolution within the plane of measurement. In order to try to create a volumetric dataset of the measurements several techniques will be attempted to combine the measurements in orthogonal directions into a single dataset. Since the measurements in either of the orthogonal directions will contain a high resolution within the plane that they are each measured they might be combined in order to obtain a more accurate dataset representing the entire volume. In theory if a flaw is detected in both orthogonal directions then the combined dataset should be able to highlight this whereas areas which do not contain any flaws should average to a lower value reducing the variation in background signal level.

In order to test this hypothesis data will be obtained of a CFRP sample that contains a side drilled hole on two orthogonal directions. Several operations on this data will be attempted to try to improve the detectability of flaws compared to the background signal levels of the measurements. The results of these operations may be reconstructed C-scans using the original FMC measurements or B-scans in one of the two planes enchanced with data measured in the orthogonal plane.

4.3. Summary

In this chapter the research questions are presented and their motivations are explained, as well as the methods by which they will be addressed.

5

Experimental

This chapter will describe in detail the experimental setup that is used for this project.

5.1. Physical components

The following components are used in the setup: Olympus Rollerprobe, Diagnostic Sonar instrument including NI PXIe chassis, PXIe-7966FPGA card, NI5752 digitizer, ABB IRB4600 robot, Robot Operating System (ROS), CFRP composite sample. The rollerprobe was chosen for its capability of moving laterally across a surface. This removes the need to create some distance between the sensor and the sample between consecutive measurements. The NI PXIe chassis, the FPGA card and digitizer were chosen to provide compatibility between the sensor and a computer which is used for the collection and processing of data. These components also all meet the bandwidth requirements to be able to process the large quantity of data that is generated by streaming FMC data. The ABB robot is selected to have a range of motion sufficient to measure the sample, as well as having enough precision to accurately position the sensor with respect to the sample. ROS is used to be able to access the robot pose in real time, allowing the location to be determined at which each measurement is taken.

5.2. Physical setup

The physical setup consists of all the individual components integrated into a single system. This integration happens on two levels, physical and digital. For the physical integration of the sensor with the robot an adapter plate is used which is designed to be attached to the robot head. This plate is a breadboard with holes spaced evenly 12.5 mm apart in the two cardinal directions. A custom T-section joint was designed to attach the rollerprobe to this plate. The rollerprobe is normally designed to be held by hand, and as such the grip is disassembled from the probe in order to free the space needed to attach it to the adapter plate. All of the connections between the sensor, joint and plate are done using M4 bolts.

In addition to the robot, the sensor needs to be attached to the PXIe in order to send the signal through the FPGA card to process them. The sensor comes with a 200 cm cable by which it connects to the PXIe chassis. Ideally this cable would be guided along the arm of the robot

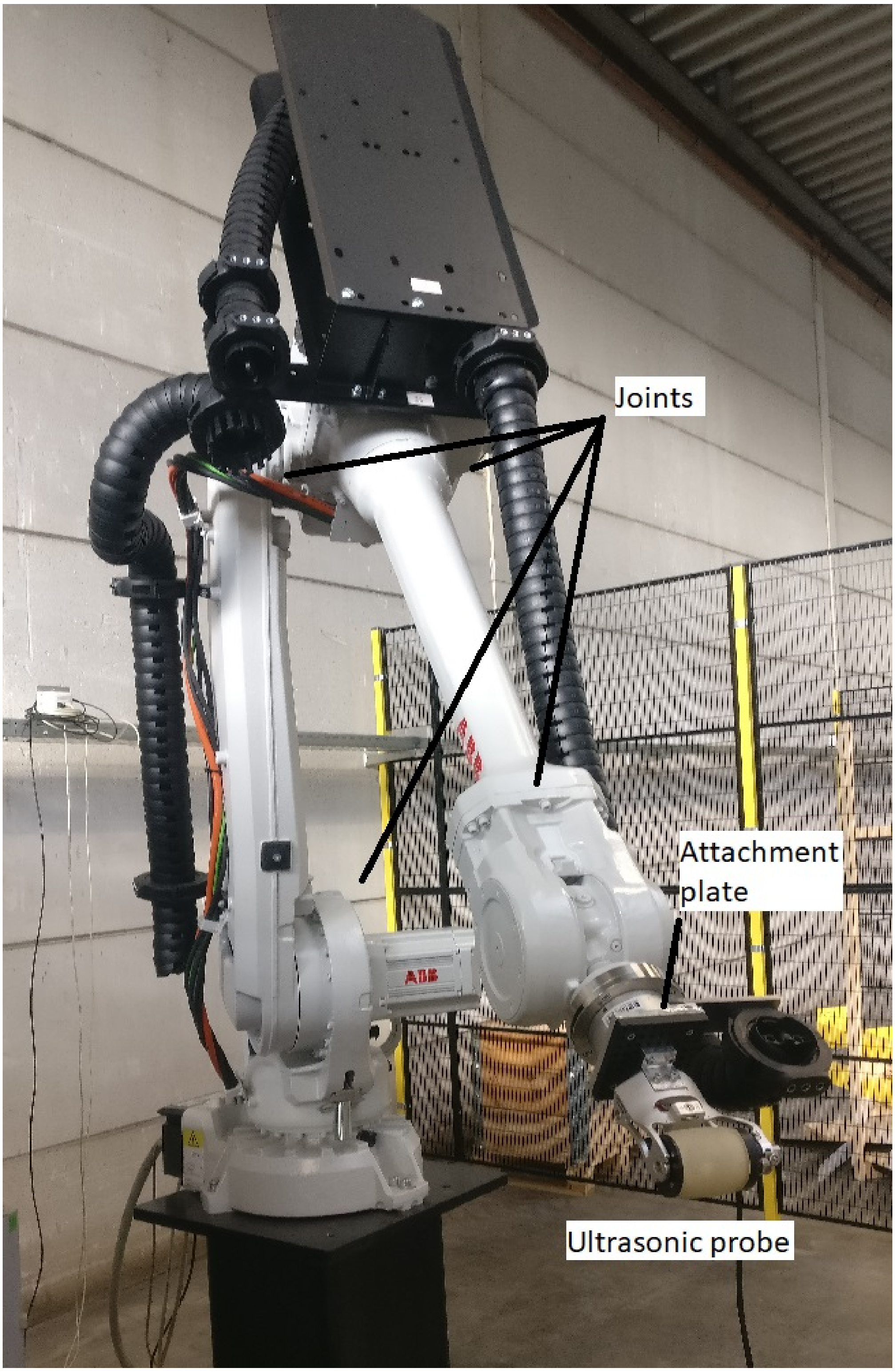
Joints
Attachment plate
Ultrasonic probe
ABB

Figure 5.1: A picture of the ABB IRB4600 robot proposed to be used for the measurement configuration. Attached to the final joint is the ultrasonic probe.

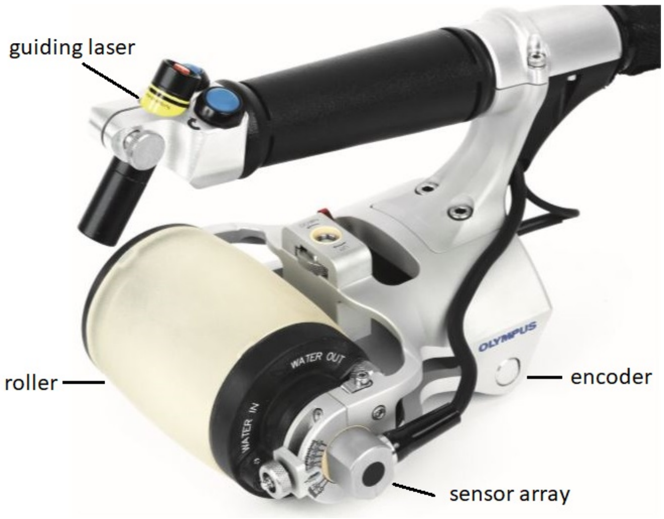

Figure 5.2: The Olympus Rollerprobe.

before connecting to the chassis to retain full freedom of motion by the robot arm. Unfortunately the current cable attached to the probe is not sufficiently long for this and thus runs directly from the head of the robot to the PXIe chassis situated a short distance away from the sample.

Inside the PXIe chassis there are two modules which are used to control the ultrasonic elements. These are the PXIe-7966 FPGA card and the NI-5752 digitizer. The combination of these two modules allows for real-time signal processing and streaming of analog data. It is these two modules that allow for the real-time capture and display of the data captured by the sensor, as well as real time processing to convert it into an image.

The sample that is used in order to acquire experimental data is selected to be representative of structures that can be found in real world applications. The sample is a flat plate with a thickness of $20mm$ consisting of plies of approximately 0.3mm per ply. The material of the plies is CFRP and it is infused with an epoxy matrix. Through the center of the plate a hole is drilled which serves as a predetermined defect which may be used to assess the quality of the scans taken of the sample. Figure 5.3 shows a picture of the sample.

5.3. Data setup

One of the limiting factors of this setup is the rate of data transfer that is needed to convey all the information captured by the probe. The size of the datasets combined with the rate at which they are collected results in a high required bandwidth. This can be particularly challenging when this data needs to be transferred across a network.

To calculate the requirements of the rate of data transfer a simple calculation can be used: the number of measurement taken per unit of time, multiplied by the number of measurements taken per capture, multiplied by the size of an individual measurement. For the current setup that calculation results in the following:

The probe consists of 64 elements, meaning that a single capture will result in 64 x 64 = 4096 measurements. Each of these measurements takes the form of a traditional A-scan between a transmitter-receiver pair. The size of one of these A-scans depends on the depth of the material

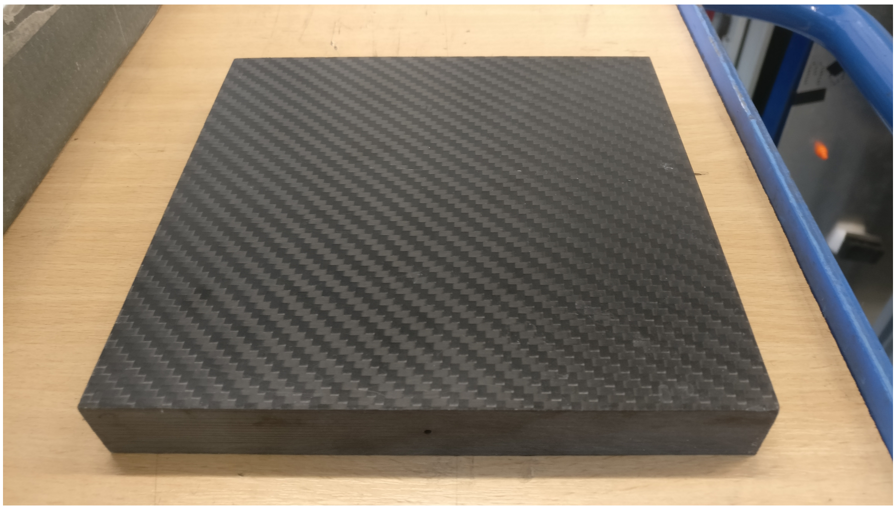

Figure 5.3: The composite sample used in the experiments

and its specific speed of sound, and for a given sample scan each A-scan was described with 252 data points. Each data point is stored in 64 bits, which means it is written using 2 bytes of information.

The resulting size of an FMC measurement can then be calculated to be 4096 x 252 x 2 / 1024 = 2016 KiloBytes. A cropped bitmap of FMC measurements can be seen in Figure 5.4, which contains measurements of the first four receiver elements in a 64-element FMC measurement. Each of the rows of pixels contains a complete A-scan between two of the elements in the array with the greyscale value indicating the intensity. Each block of 64 rows contains all the information captured by a single receiver element.

Overhead for this data exists in the form of the configuration options of the sensor, as well as position data at which the measurement is taken. This overhead takes up several KiloBytes of information, which can be observed as the difference between the calculated size of the dataset and the observed size of 2024kB. The configuration options for the measurements remain the same throughout the run and can therefor be neglected in the overall data rate calculations.

The PXIe chassis used in the setup has a hardware limit of 250 MB/sec, which translates to a theoretical maximum rate of capture of 125kHz. This value can be increased by using a different PXIe chassis which supports a different method of data transfer, but this value is higher than the rate at which the sensor can capture and should therefor suffice.

5.4. Experimental capture

The process of obtaining a measurement from a sample will be done as follows. The sample would be attached to the bed using double sided tape in order to keep the top surface free for access by the probe. A robot path would be determined based on either the dimensions of the plate or a CAD model in the case of a more complex geometry. This robot path is defined from a starting point on the plate, and before the capture commences the robot would be positioned on the determined starting point of the path across the plate. For this experiment a simple flat panel is used as a specimen, which means the path planning of the robot was kept as simplistic as possible. A starting point was defined from which the sensor moves in a straight line without changing the height of the probe. This process could be adapted for more complex

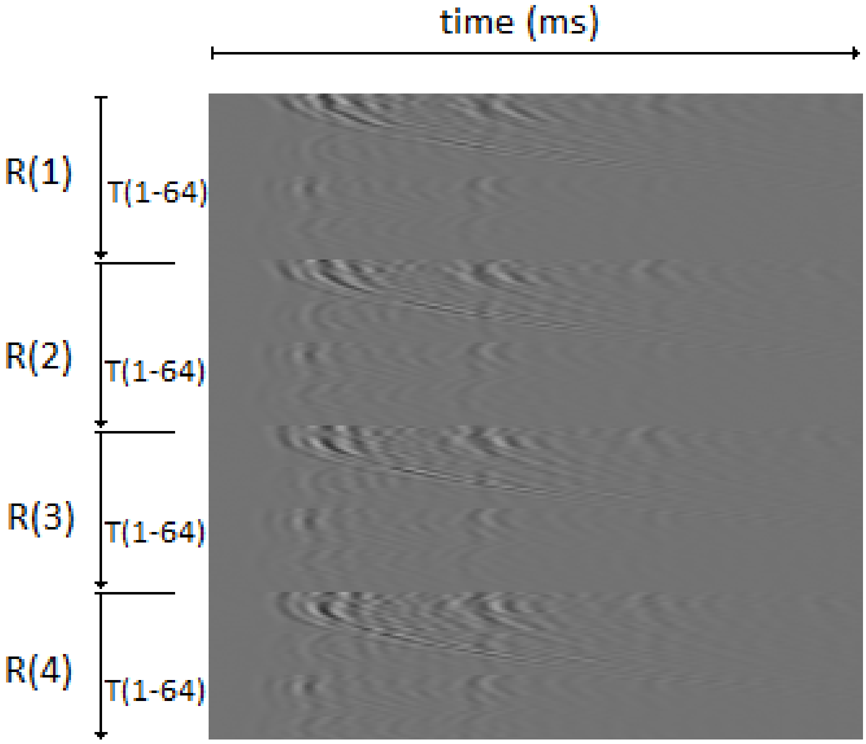

Figure 5.4: A cropped bitmap containing data from the first 4 receivers in a 64 element FMC measurement. The data is structured such that measurements between all the transmitting elements T(1)-T(64) are displayed for the first receiver R(1) in each of the consecutive rows. This is then followed by the measurements between T(1)-T(64) for the second receiver R(2), etc. Values are represented in greyscale with a value between 0 and 255 and represent normalized A-scans.

geometries, however the suggested method would not just consist of a simple feed forward loop moving the end effector to a given position. Instead a feedback signal of a pressure sensor would be integrated into the control loop in order to control the normal force between the sensor and the sample. The normal force between the sensor and the plate is not only important in order to prevent damage to the probe, but also to ensure consistent signal strengths, as poor contact between the probe and the sample would result in a higher acoustic impedance and thus affecting the output signal.

Once the capture commences the capturing software will take timed captures at a set interval such that each capture occurs at a specified location. The exact location of each capture can be retrieved from ROS [43], which keeps track of the exact pose of the robot at a given time. Ideally the sensor data would also be transmitted through ROS however due to compatibility issues of the capturing software with open source modules for integration this step is forfeited in the actual experiment.

The end result of the capture should be a set of FMC measurements and their corresponding coordinates in 3D space to allow for reconstruction of the measured volume. Each of these FMC measurements will need to undergo post-processing in order to translate it from a bitmap containing the A-scans that comprise the FMC measurement to an intensity map of 2D frames of the volume underneath the probe. The post-processing is commonly referred to as the total focusing method (TFM) and is currently done in a script written in MATLAB, this process is described in section 3.2.7. The combined data with their associated positional coordinates can then be combined into a volumetric dataset representing the complete sample. The possibilities of what this data can be used for is investigated in chapter 6.

5.5. ROS Integration

It was originally intended to integrate the diagnostic output data stream with the ROS environment. Two designs were attempted to be implemented. The first design was to directly send the output datastream from the Diagnostic Sonar software to ROS, to then integrate the data with the most recent sensor positioning data. This however ran into the issue that the data streaming was unstable and not properly adhering to software commands it was given. The second design was to integrate an open source module called ROS-for-Labview directly into the source code of the Diagnostic Software Sonar. Although this method was promising the Diagnostic Software sonar manually overwrote the network port used for communication to the ROS node. Where this port was overwritten could not be found in the software and thus the idea was not further pursued.

Unfortunately the Diagnostic Sonar company went out of business during the project period. This led to no further software updates being issued and limited technical support. An external contractor was engaged to fix this problem and was also unable to solve the integration issues. Because of this it was not possible to proceed further on this sub research question.

5.6. Conclusion

This chapter discusses the components used for the experimental setup. It discusses the physical configuration of the various components that comprise the system as well as the way in which they are connected. An investigation of the data output is discussed and implications it has on the rate of data capture under ideal conditions. Furthermore the integration process of the output datastream with the robot positioning data is discussed.

6

Results & Analysis

This chapter will discuss the data captured during the experiment and the proposed operations in order to analyze and enhance this data.

6.1. Individual FMC

A single measurement takes the shape of a section view of the measured object of 51.2mm in width by its depth of 20mm. This section view is reconstructed from the raw FMC measurement by using the TFM algorithm as described in section 3.2.7. The width of the image is directly related to the width of the linear array of ultrasonic elements, which consists of 64 elements with a width of 0.8mm each. An example image from one of the datasets is shown in Figure 6.1.

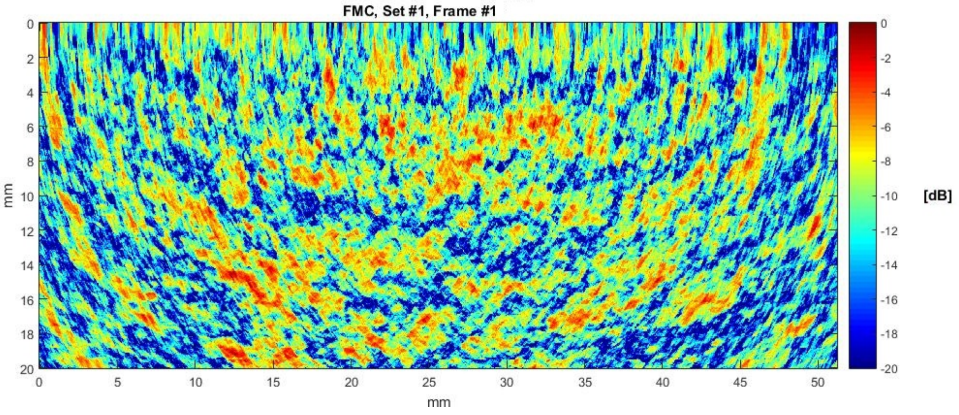

Figure 6.1: An individual FMC measurement formatted using the TFM algorithm

The dataset is constructed with a resolution of 32 data points per millimeter in the plane of the measurement. Each point is attributed a value according to the calculated acoustic impedance as per the TFM algorithm. The values obtained for each frame are normalized to a maximum value of that frame and represented on a logarithmic scale.

One observation that can be made from looking at the raw data is that the image is slightly distorted towards the edges of the measurement. An explanation for this distortion would be that as one moves further from the center of the image the majority of the elements will observe the location under a high angle. A point on exactly the edge of the image will be constructed entirely from measurements on only one side of this point, while a point in the center will have a more balanced perspective from both sides.

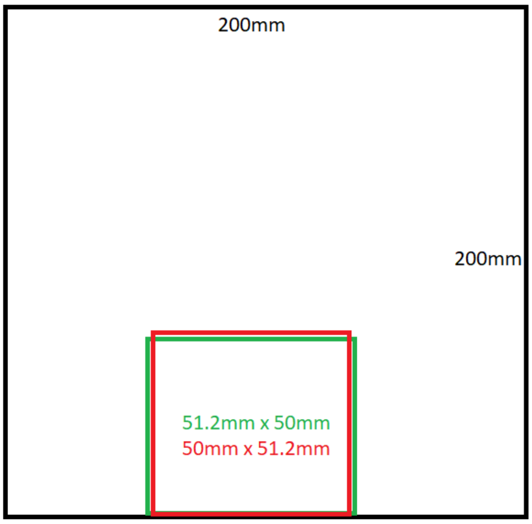

Figure 6.2: Measurement location with respect to the panel

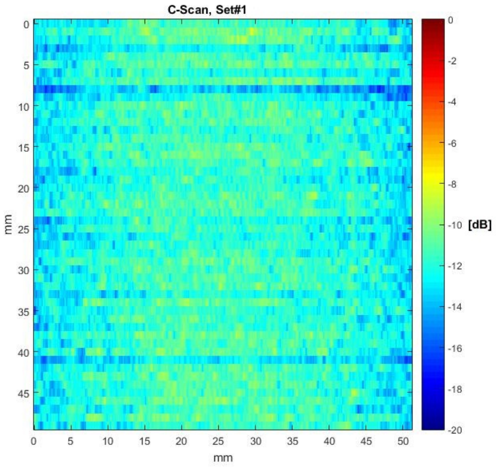

Figure 6.3: Reconstructed C-scan of dataset 1

6.2. Comparing the Data Sets

The experimental data consists of two series of FMC scans covering a 50mm distance with a 1mm spacing. These two datasets are taken orthogonal to each other centered around the same point. The area on the sample that is measured is indicated on Figure 6.2. The two resulting datasets then each cover a 51.2mmx50mmx20mm volume with a resolution of 32x32x1 datapoints per millimeter. By taking the average value across the depth these two datasets can

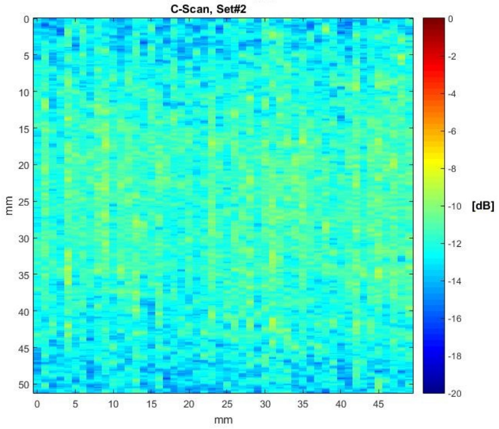

Figure 6.4: Reconstructed C-scan of dataset 2

be represented as C-scans as displayed in Figures 6.3 and 6.4.

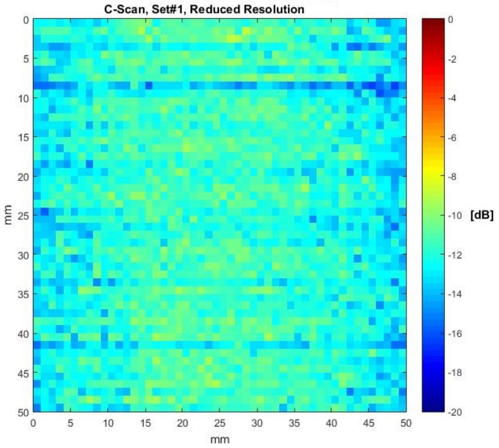

Figure 6.5: Reconstructed C-scan of dataset 1 at reduced resolution

By trimming these two datasets they can be reduced to an overlapping 50mmx50mm area. In order to compare these two datasets their resolution will be reduced from 1600x50 to 50x50 by taking the average value of 32 points. These two C-Scans can be seen in Figures 6.5 and 6.6.

A combined image can be created by averaging the value of each data point. This combined C-scan is displayed in Figure 6.7.

What can be observed from the two reduced C-scans is that the average intensity towards the edges of the probe is much lower than the average intensity near the center of the probe. The difference between the two datasets can be observed in Figure 6.8 which highlights the difference between the measurements in the two directions near the edges of the measurement. Since the sample consists of a uniform plate the expected result would be for the data to have the same average intensity across the entire plate.

The difference in average between the two datasets is only 0.01dB, with an average absolute difference of 1.27dB between the two sets. The minimum and maximum differences observed

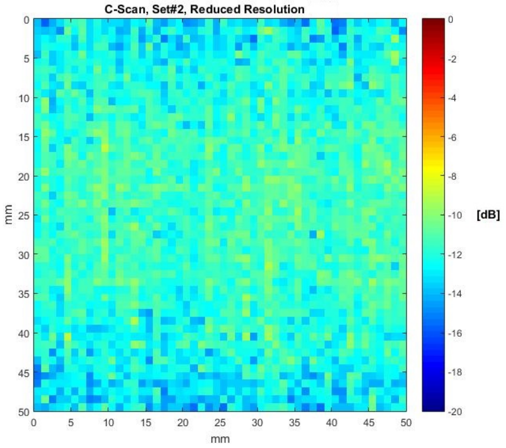

Figure 6.6: Reconstructed C-scan of dataset 2 at reduced resolution

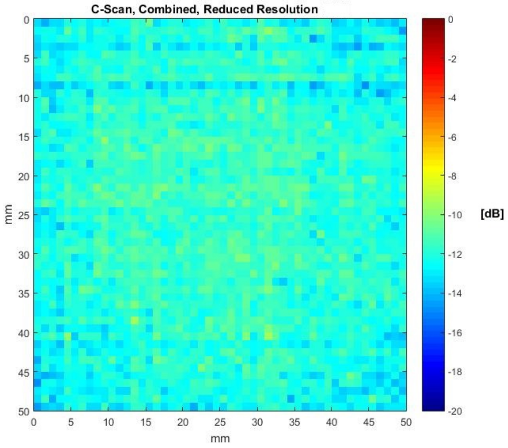

Figure 6.7: Average of the two C-scans at reduced resolution

between these C-scans are -6.35dB and 5.6dB respectively.

6.3. Enhancing the resolution

By combining the two datasets a single dataset can be created of a higher resolution than the original datasets. This is done by taking the average value of two datasets at every point in a 1600x1600 grid. Since the original resolution was 50x1600 for either dataset, this means that each of the 50 measurements has to be reused 32 times for each datapoint measured in the orthogonal direction.

The data at improved resolution show a similar shape to the data at reduced resolution. The edges of the measurements result in the largest differences between the two datasets similar as was observed with the reconstructed C-scans at reduced resolution. The difference in average between the datasets at improved resolution is 0.005dB with an absolute difference in average between the two datasets of 1.26dB. The minimum and maximum values observed for the differ-

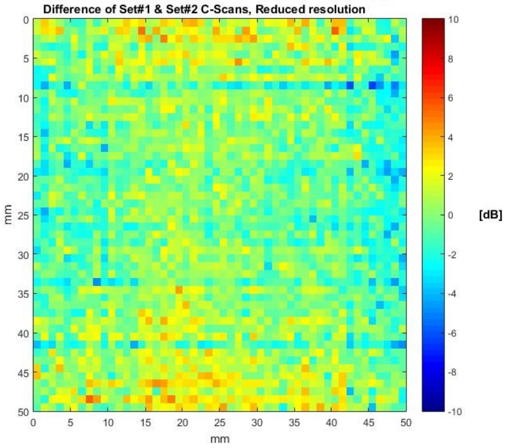

Figure 6.8: Difference of the two C-scans at reduced resolution

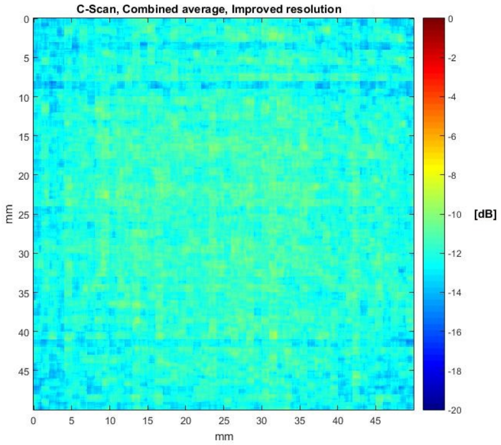

Figure 6.9: Average of the two C-scans at improved resolution

ence between these C-scans are -7.76dB and 6.66dB respectively. As would be expected the minimum and maximum values for the difference between the two sets is higher than observed for the datasets at reduced resolution, however the average differences observed are nearly identical.

6.4. Analysis of the data

The accuracy of the measurements needs to be assessed by how well the measurement conforms to the expected shape of the data. The sample consists of a uniform plate with a small hole drilled into the side of the sample, as seen in Figure 5.3. This hole has a diameter of 0.5mm and a depth of 10mm and should therefore be observed in the measurements. Observing Figure 6.1 however does not reveal this manufactured defect, which should appear in the middle of the image.

Looking at the reconstructed C-Scans an interesting observation can be made. Dataset 1 con-

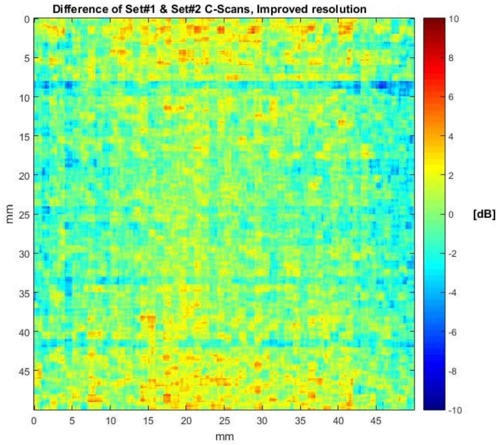

Figure 6.10: Difference of the two C-scans at improved resolution

tains two measurements that have a significantly lower average than the rest of the measurements. This can be explained by the method by which values for the individual FMCs are converted to intensity values. When a FMC measurement is converted to intensity values for each point using the TFM algorithm the values are normalized to the highest value in the set. This means that if one FMC contains one extreme value compared to the rest of the values within that measurement the rest of the values within that measurements will be scaled down.

Although it appears that by taking the average of the two sets such anomalous measurements can be averaged out this may in fact be undesirable. What could be an indication of a more extreme value existing within one of the FMC measurements in fact gets hidden behind the average between the two sets. Only if in both directions a higher average can be found in a certain location will this location show up as a hot spot in the image. Even when this is the case the intensity value at this location may not be significantly higher than the rest of the dataset if other FMC measurements result in a more uniform result, which should on average yield higher values. One possible solution to this problem would be to normalize all the FMC measurements to the same value.

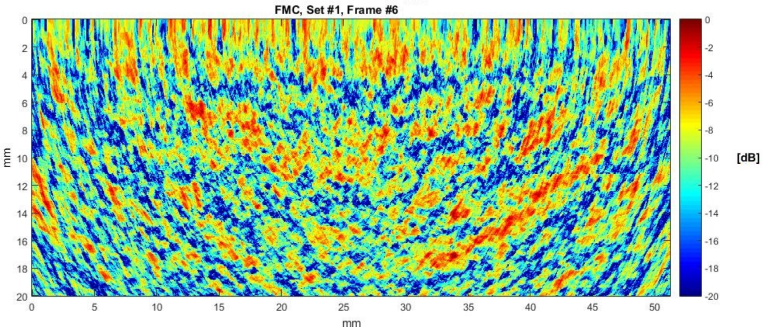

Figure 6.11: FMC measurement of frame 6 of the first dataset

To take a closer look at why frame 7 of the first dataset provides such a different result for the averaged values displayed in the C-scan frames 6 to 8 will be displayed and compared in Figures 6.11, 6.12 and 6.13. Comparing these three images shows that frame 6 and 8 contain high values of accoustic impedance towards the top edge of the measurement. The absence

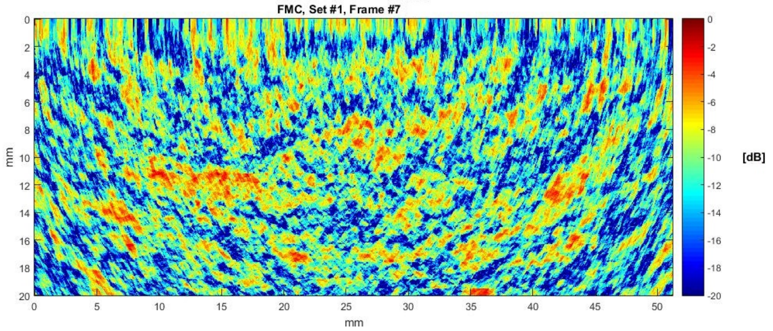

Figure 6.12: FMC measurement of frame 7 of the first dataset

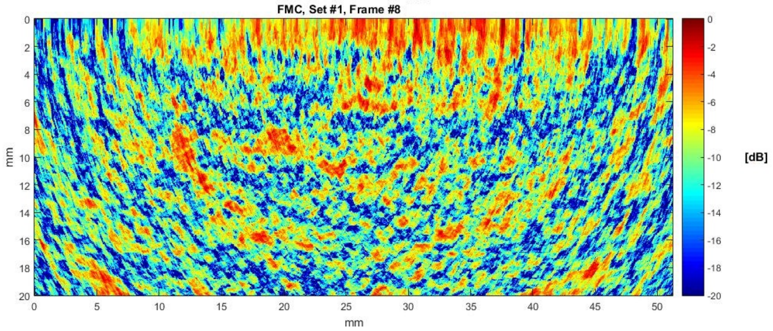

Figure 6.13: FMC measurement of frame 8 of the first dataset

of these high values towards the top edge of the measurement in frame 7 means that although towards the center of the sample the measurement values approach similar values, the average value across the depth turns out significantly lower than for the adjacent frames. This seems to be largely attributed to the noisy nature of FMC data taken of samples made of composite materials.

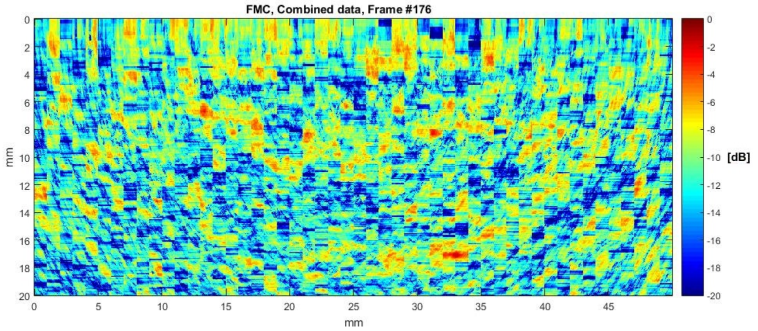

Figure 6.14: Combined FMC measurement of frame 6 of the first dataset with the second dataset

In order to get a better understanding of how combining the data affected the FMC data the equivalent of frame 7 in the first dataset is plotted after it was combined with the second dataset. The combined frames equivalent to frames 6 7 and 8 of the original dataset 1 are displayed in Figures 6.14, 6.15 and 6.16. One clear observation that can be made from this is that the resulting data is not continuous. Discrete jumps in values can be seen at the intersections of each orthogonal measurement as it is combined with the data of the first set, however the variation in peak values near the edges are reduced.

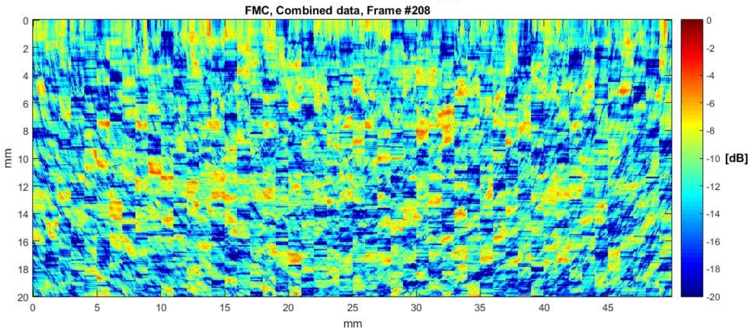

Figure 6.15: Combined FMC measurement of frame 7 of the first dataset with the second dataset

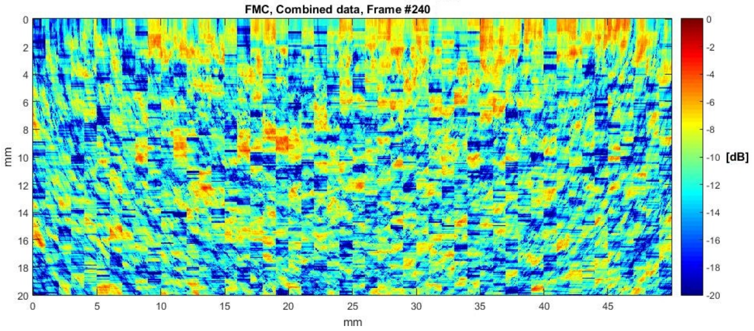

Figure 6.16: Combined FMC measurement of frame 8 of the first dataset with the second dataset

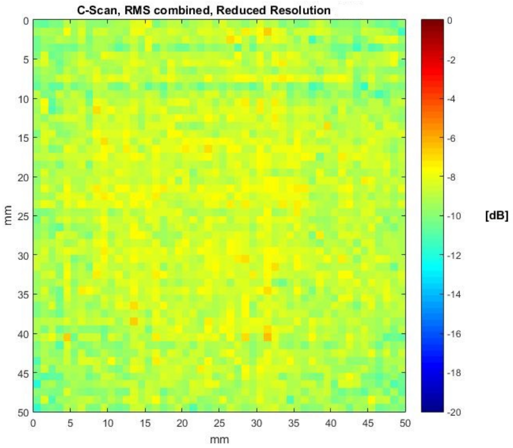

Figure 6.17: RMS of the two C-scans at reduced resolution

6.5. Alternative methods for data combination

Taking into account the fact that data is normalized to the highest value within a frame, other methods might be more useful to combine the data of the 2 sets. One suggested method for combining the data is to take the root mean square of the different values rather than the average. Taking the root mean square will result in an emphasis towards the higher of the two values, which should in theory result in a measurement that contains a larger focus on locations where defects may be present.

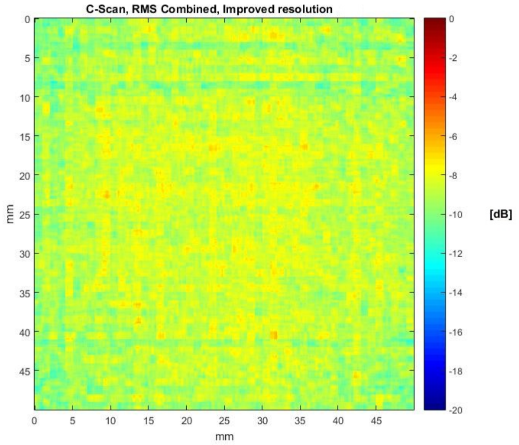

Figure 6.18: RMS of the two C-scans at improved resolution

In order to take the RMS value of the two datasets each value is first converted from its logarithmic scale back to linear scale, where the RMS value is taken before converting back to decibels. The resulting images of the reduced and improved resolution datasets are shown in Figure 6.17 and 6.18. Using this method one clear difference can be observed compared to the images created using the average between the two dataset. The average of the values found using this method is 3dB higher. The information contained in this plot is however contained in the variation in the values across the plot, so this data should be assessed in how well high values from the original two datasets can be observed in this combined image. Comparing these figures to Figure 6.7 and 6.9 shows that hot spots can be found in similar locations to the average based combined datasets. This method also somewhat normalizes the low average frames from the first dataset, which results in an overall more uniform plot. Although this does better represent the uniform material of the composite sample, it remains unclear from this whether this obfuscates actual defects or not.

6.6. Conclusions

The original FMC measurements used to create these datasets contain a large variation in calculated acoustic impedance, as a result it is fairly difficult to make out individual defects within the material by taking averages of these values. Distortions of the measurements towards the edges of the array as well as peak values near the top and bottom interfaces of the material also result in peaks in measurements. These peaks may cause actual defects to go undetected due to these peaks having values in the same order as defects would have. Combining the two measurements in two directions does allow for the creation of a single dataset at much higher resolution than would otherwise be possible using the same number of measurements, however the quality of these measurements would need to be improved before this method can be used to more accurately detect defects.

7

Discussion

The objective of this research was to improve the quality of ultrasonic measurement data taken using FMC by combining measurements in orthogonal directions. The research assumes that a large number of measurements are taken in an automated fashion which allows their location to be determined in advance. This location data can be used to reconstruct the measurements into a volumetric dataset which could in theory increase the information obtained about a measured sample.

The sample that was used to take the measurements contains a manufactured defect, which is a hole drilled into the side. According to ultrasonic theory the dimensions of this hole should fall within the range where it can be detected using this method, however this hole could not be detected on the measurement data. A potential explanation for this could be the type of probe that was used, this probe consists of a linear array of ultrasonic elements contained within a silicone wheel which is filled with water. The silicone wheel has a tendency to deteriorate over time when exposed to water, which can be observed by the silicone rubber turning from its translucent color to an opaque yellow-white. This may result in degraded acoustic properties and is mentioned in the manual of the equipment. At the time of taking the measurements this degradation has been observed on the sensor equipment and this may have contributed to the variation in measured acoustic impedance.

Another prediction of the data was that it should return somewhat uniform values for all the measurements, as the sample that was used in the experiment was a pristine CFRP sample outside of the manufactured defect. This is clearly not the case as effects towards the top edge of the material tend to cause the values peak there, while values near the edges of the sensor appear distorted and generally consist of lower values. Large variations in the measurements are however found throughout the material, not just near the edges. A possible explanation for this is reflections caused by the laminar nature of CFRP. As the sample consists of a number of plies of fibers under various angles, the interface between these layers can result in scattering of the signal which results in the noisy nature of the signal.

The measurements taken using this method can be compared with another FMC measurement of a sample containing a large delamination. An example of such a measurement can be seen in Figure 3.6b with Figure 3.6a to be used as a comparison of a measurement of the same sample without a delamination. When also comparing these measurements to Figure 3.5b which displays an FMC measurement taken of a homogenous material a clear difference in the shape of the data can be observed. The difference between FMC data taken of composites and homogenous materials highlights the difficulty in analyzing composites using ultrasonic techniques. Even when a large defect is present in the material interpretation is needed in order to confirm its presence.

8

Conclusions & Recommendations

In this chapter the conclusions and recommendations drawn from this research are presented.

8.1. Conclusions

This research proposes the use of an ultrasonic phased array sensor in combination with a multi degree of freedom robotic arm in order to take large datasets of FMC measurements. It attempts to answer the question if automated FMC can be used to inspect composite parts. This is further divided into two subquestions: Can FMC be used in conjunction with Robotics to scan fiber laminate composite materials? and Can orthogonal datasets be used to improve the probability of detection of FMC data measured of composites?

The physical combination of an ultrasonic probe with a robotic arm was proven possible with the use of a roller-probe which contains a linear array of ultrasonic elements contained in a silicone rubber wheel filled with water which acts as a medium to transmit the ultrasonic pulses to the material.

Besides the probe the ultrasonic equipment consists of a large chassis containing hardware used to interface the probe with a computer which is used to extract and store the data. Besides the interfacing hardware this chassis contains an FPGA as well as a digitizer in order to access and operate on the data in real-time, as well as to modulate the signal to be sent to the probe. Integration of this chassis with the robot is difficult due to its relative size. The probe attaches to this chassis with a cable that has a length of 200cm, which severely limits the freedom of motion of the robot if the chassis is mounted separate from the robot as it was in this case. At this time use of a longer cable is not possible due to technical constraints, as the one currently used it already approaching the maximum length for such a connection. If this cable were made any longer it would negatively affect the signals that are transmitted through it, since the individual voltages of the elements are low and thus susceptible to interference.

The sensor being of the roller-probe type is important to be able to use it in combination with a robot for several reasons. Firstly the roller being made of silicone rubber means there is some flexibility in the positioning of the sensor with respect to the sample. Since the stiffness of this roller is relatively low there is a smaller chance of damaging either the probe or the material when positioning the probe on the sample using robotics. Furthermore because the probe is of a roller type it means the probe only needs to be moved to touch the sample once, and can be moved parallel to the surface when contact is established. For a flat sample this has the additional benefit that all measurements are taken with the same normal force, which affects the distance between the probe and the sample, as well as the conductivity of the ultrasonic waves from the water through the silicone into the sample. This conductivity affects the signal strength due to the acoustic impedance being lower if proper contact is made. In order to further improve this contact the interface between the probe and the sample should be coated in water. This should reduce signal loss due to acoustic impedance of the interface.

Two datasets are taken of a 50mmx50mm area of a CFRP laminate that has a thickness of 20mm. Datasets would be constructed with the use of position data provided by the robot into volumetric datasets representing the sample. These two datasets overlap the same area and are taken in orthogonal directions. Because FMC measurements contain more information in the plane of the sensor these two datasets are used to complement each other in the direction where they have a low resolution. The resulting dataset that is created contains a much higher resolution compared to the original dataset.

The original datasets have a size of 50x1600x500 datapoints, and by combining them a dataset can be created that contains 1600x1600x500 datapoints. This means that by taking twice the number of measurements the resolution of the data was increased by a factor of 32. This number may vary depending on the configuration of the FMC measurement as well as the parameters used to perform the TFM algorithm.

Unfortunately a feature of ultrasonic measurements of composite materials is that they result in very noisy signals. This can be attributed to the laminar nature of the material and reflections this may cause at ply intefaces. As a result defects at a resolution where they should be detectable in theory are drowned out by the noise. An example of this is a manufactured defect in the sample, a 0.5mm diameter hole drilled in the side of the sample can not be detected by measurements in either direction.

The combined datasets appear to average out the peaks that occur due to the variation in material density. One benefit of combining the orthogonal data that can be observed is that more accurate measurements can be taken in near the edges of the probe where the constructed image appears to distort. If the data were cropped to exclude this distorted data approximately 10mm would have to be cropped from either side of the measurement for this probe. The usable area of a 50mmx50mm dataset would have therefor have to be reduced to approximately 50mmx30mm in order to crop the distorted data out.

In conclusion the techniques proposed in this research appear to be feasible, but should be combined with other methods of data processing in order to obtain more comprehensive results.

8.2. Recommendations

The first and foremost recommendation is to try to combine this method of data fusion with a method that takes into account the internal structure of the composite material. If an algorithm were used in order to take into account the reflections of the signal cause by the different plies some of the noise could be reduced from the measurements thus allowing for the detection of smaller size flaws in a sample. Recent research has been published presenting such a method. [45] This is of importance since the defect that was introduced into the sample was of a size large enough to affect its mechanical properties. Alternatively machine learning algorithms can be investigated for the detection of flaws in the large quantitiy of data that is produced by this method.

Some of the limitations of this method appear to originate from the fact a roller-probe was used. One of these limitations is the minimum thickness of the sample, which is currently 20mm. Another is the potential scattering of the signal due to a less direct interface with the material compared to a probe in direct contact with the material. It would be beneficial to see if the size of detectable defects may be lower using a conventional ultrasonic array in direct contact with the sample.

Although this method was developed for composite materials it would be interesting to see how this method behaves for homogenous materials. Measurements of homogenous materials contain a lot less background noise and don't contain large spikes in values near the top and bottom interfaces of the material. As a result they should be much more suitable for the data combination techniques used in this research.

Bibliography

[1] Christos Kassapoglou. Design and analysis of composite structures with applications to aerospace structures. book, pp. 1-7, 2013.

[2] T. Skinner and S. Datta and A. Chattopadhyay and A. Hall. Fatigue damage behavior in carbon fiber polymer composites under biaxial loading. Composites Part B: Engineering, vol. 174 , no. 106942, 2019.

[3] Dongfeng Cau and Haixiau Hu, and Yao Wang, and Shuxin Li. Experimental and numerical studies on influence of impact damage and simple bolt repair on compressive failure of composite laminates. Composite Structures, Vol. 275, no. 114491, 2021.

[4] Wincheski M. Namkung, B and Padmapriya N. Ndt in the aircraft and space industries. Reference Module in Materials Science and Materials Engineering, 2016.

[5] M. Talvard. Ndt techniques: Eddy current techniques. Encyclopedia of Materials: Science and Technology (Second Edition), pp.6011-6015, 2001.

[6] U. Zscherpel S. Kolkoori, N. Wrobel and U. Ewert. A new x-ray backscatter imaging technique for non-destructive testing of aerospace materials. NDT and E International, vol.70, pp.41-52, 2015.

[7] D. Lovejoy. Ndt techniques: Penetration of liquids. Encyclopedia of Materials: Science and Technology (Second Edition), pp.6024-6026, 2001.

[8] K. Goebbels. Surface crack detection by magnetic particle inspection. Materialprufung, Vol. 30, No. 10, pp. 327–332, 1988.

[9] C. Payan, O. Abraham, and V. Garnier. Non-destructive testing and evaluation of civil engineering structures. book, pp. 23, 2018.

[10] M. Effing. Expert insights in europe's booming composites market. Reinforced Plastics vol.62, Issue 4, pp.219-223, 2017.

[11] D.K. Hsu. Non-destructive evaluation (nde) of aerospace composites: ultrasonic techniques. book, pp. 397-422. 2013.

[12] Bercli. Full matrix capture (fmc) and total focusing method (tfm). `http://bercli.net/documentation/article_FMC&TFM.htm`, 2005.

[13] S.Ramakrishnan J. Frketic, T. Dickens. Automated manufacturing and processing of fiber-reinforced polymer (frp) composites: An additive review of contemporary and modern techniques for advanced materials manufacturing. Additive Manufacturing, vol.14, pp.69-86, 2017.

[14] Richard Kruithof and Roger M. Groves. Literature study: Automated inspection using phased array ultrasonics. TU Delft, 2019.

[15] S.Ramakrishnan J. Frketic, T. Dickens. Automated manufacturing and processing of fiber-reinforced polymer (frp) composites: An additive review of contemporary and modern techniques for advanced materials manufacturing. Additive Manufacturing, vol.14, pp.69-86, 2017.

[16] S. Mazumdar. Composites manufacturing, materials, product and process engineering. CRC Press LLC, 2002.

[17] D. Lodha Z. Burt, A. Bortz. Cnc milling. `http://www.cs.cmu.edu/~rapidproto/students.03/zdb/project2/CNCmain.htm`. Accessed 06-02-2019.

[18] M.K. Dhadwal and S.N. Jung. Free-edge stress evaluation of general laminated composites using a novel multifield variational beam formulation. Composite Structures, vol. 233, no. 111705, 2020.

[19] P. Mertiny R. Henriquez. Reference module in materials science and materials engineering. Comprehensive Composite Materials II, vol. 3, pp. 556-577, 2018.

[20] J. Carey. Handbook of advances in braided composite materials, theory, production, testing and applications. Woodhead Publishing, 2017.

[21] R.McIlhagger A. McIlhagger, E.Archer. Polymer composites in the aerospace industry. Woodhead Publishing, 2015.

[22] M. Jonsson A. Björnsson and K. Johansen. Automated material handling in composite manufacturing using pick-and-place systems - a review. Robotics and Computer-Integrated Manufacturing, vol. 51, pp. 222-229, 2017.

[23] L. Zhang W. Xu. Tool wear and its effect on the surface integrity in the machining of fibre-reinforced polymer composites. Composite Structures, vol. 188, pp.257-265, 2018.

[24] R. Principe, L.M. Vallejo, J. Bailey, R. Berthet, L. Favier, L. Grand-Clement, and F. Savary. Phased array ultrasonic nondestructive tests of soldered current-carrying bus-bar splices of superconducting magnets. IEEE, 2018.

[25] NDT Resource center. Ndt method summary. `https://www.nde-ed.org/GeneralResources/MethodSummary/MethodSummary.htm`. Accessed 27-06-2018.

[26] R. Groves R. Tonnaer and S. Schroff. Preventitive online nde in afp. Proceedings of the Third International Symposium on Composite Manufacturing (pp. 114-123)), 2017.

[27] G. Dib, S. Roy, P. Ramuhalli, and J. Chai. In-situ fatigue monitoring procedure using nonlinear ultrasonic surface waves considering the nonlinear effects in the measurement system. Nuclear Engineering and Technology, 2019.

[28] F. Bentouhami, B. Campagne, E. Cuevas, T. Drake, M. Dubois, and T. Fraslin. Lucie - a flexible and powerful laser ultrasonic system for inspection of large cfrp components. LU2010, 2010.

[29] Sahu O.M., Balabantaray B.K., Patle B., and Biswal B.B. Part recognition using vision and ultrasonic sensor for robotic assembly system. IEEE, 2015.

[30] V. Kappatos, G. Asfis, K. Salonitis, V. Tzitzilonis, N. Avdelidis, E. Cheilakou, and P.Theodorakeas. Theoretical assessment of different ultrasonic configurations for delamination defects detection in composite components. Procedia CIRP, vol.59, pp.29-34, 2017.

[31] G. Dobie, W. Galbraith, C. MacLeod, R. Summan, S.G. Pierce, and A. Gachagan. Automatic ultrasonic robotic array. IEEE, 2013.

[32] C. Mineo, C. MacLeod, M. Morozov, S.G. Pierce, T. Lardner, and R. Summan. Fast ultrasonic phased array inspection of complex geometries delivered through robotic manipulators and high speed data acquisition instrumentation. IEEE, 2016.

[33] R. Crane. Radiographic inspection of composite materials. Comprehensive Composite Materials II, vol.7, pp.167-194, 2018.

[34] V. Kumar, T. Yokozeki, T. Okada, Y. Hirano, T. Goto, T. Takahashi, and T. Ogasawara. Effect of through-thickness electrical conductivity of cfrps on lightning strike damages. Composites Part A: Applied Science and Manufacturing, vol.114, pp.429-438, 2019.

[35] G. Ferrano K. Goebbels. Automation of surface defect detection and evaluation. Non-Destructive Testing, pp.2762-2773, 1988.

[36] R. Thompson and S. Begum. Ndt techniques: Ultrasonic. Reference Module in Materials Science and Materials Engineering, 2017.

[37] Olympus. An introduction to ultrasonic phased array technology. `https://www.olympus-ims.com/en/ultrasonics/intro-to-pa/`. Accessed 09-07-2018.

[38] Olympus. Material sound velocities. `https://www.olympus-ims.com/en/ndt-tutorials/thickness-gauge/appendices-velocities/`. Accessed 09-07-2018.

[39] J. Peng, H. Peng, Y. Zhang, X. Gau, C. Peng, and Z. Wang. Study on the railway wheel ultrasonic inspection method using the full matrix capture. IEEE, 2013.

[40] ABB. Irb 4600 industrial robot. `https://search.abb.com/library/Download.aspx?DocumentID=ROB0109EN_G&LanguageCode=en&DocumentPartId=&Action=Launch`, 2020.

[41] ABB. Irb 4600 industrial robot. `https://new.abb.com/products/robotics/robotstudio`, 2021.

[42] Z. Zhijian, C. Youping, D. Zhang, J. Xie, and M. Liu. A six-dimensional traction force sensor used for human-robot collaboration. Mechatronics, Vol. 57, pp.164-172, 2019.

[43] ROS. Ros core components. `https://www.ros.org/core-components/`, 2021.

[44] C. Mineo, C. MacLeod, M. Morozov, S.G. Pierce, R.H. Brown, and J. Riise. Assessing the accuracy of industrial robots through metrology for the enhancement of automated non-destructive testing. IEEE, 2016.

[45] Chirag Anand, Roger M. Groves, and Rinze Benedictus. Modeling and imaging of ultrasonic array inspection of side drilled holes in layered anisotropic media. Sensors, vol. 21, no. 14, 2021.